Investigating the Solar Potential in Mekelpark

E.J. Roosenbrand

Bachelor Thesis

Supervisors:
Dr. R.C. Lindenbergh
Dr. M. Schleiss

Coordinator:
Dr. K.H.A.A. Wolf

Faculty of Civil Engineering and Geosciences TU Delft
31/10/2017

Abstract

The newly developing world of green energy is growing at an increasingly rapid pace. With wind turbines causing increasing tensions in communities relating to skyline pollution and debates about their net effectiveness, solar panels seem like the most effective, cheap and universally applicable solution.

In this world of increasingly sustainable energy generation, the TU Delft 'recognizes the imperative need to transition towards holistically sustainable systems.'[1] What better way to keep this promise than by investing on its own campus into a relatively low cost and high effectiveness green-energy solution?

Traditionally, light poles are powered by the electrical grid. In remote places where electricity may not be available, a popular alternative is to rely on solar energy and photovoltaic cells. FlexSol is a young Delft-based company that develops flexible solar cells that can be embedded in sheets and bended around poles or incorporated in roof tiles, bringing light and power to many places around the world. There is, however, one important issue with solar energy: it requires a minimum amount of sunlight to work properly!

Since solar panels require a high investment, determining how much energy they will produce is important before placement. Also from an environmental perspective it is beneficial to place these poles in the most optimal position, since their production also has an environmental impact. In this thesis the solar potential of a specific section of the TU campus, the Mekelpark, will be investigated. This will be calculated in three phases using both spatial and meteorological information. This will provide FlexSol with a strategy for where to place solar powered streets poles.

First, the amount of hours of sun at a certain location will be calculated, according to the geometry of the situation. Then, using KNMI data, this calculation will be adjusted for average weather conditions. This will generate a model of the expected kW per day for an area of the Mekelpark.

As was anticipated, the amount of kW per day varies throughout the seasons, not only because the sun intensity varies, but because the sun doesn't reach as high throughout the year. As a result of sun light hour calculations, the percentage hours of sunlight compared to a shadow-less location range from 42% to 88%. For the results of the kW per day as a percentage of a shadow less location, ranges from 33% to 40%.

Acknowledgments

I would like to thank my supervisors, Dr. Roderik Lindenbergh and Dr. Marc Schleiss for their support, in making this thesis happen. I would also like to thank the FlexSol company for their useful information.

Esther Roosenbrand

Delft, October 2017

Table of Contents

Chapter 1: Introduction

The goal of this report is to determine the solar potential at the Mekelpark. This solar potential is dependent upon several factors; which are deterministic and stochastic. Deterministic factors include; Earth orbit and rotation, variation in latitude and longitude, terrain, buildings and shadows cast by these objects as well as the features of solar cells (inclination, orientation and efficiency). Stochastic or dynamic factors include; weather and variations in atmosphere contents (gases and aerosols), presence of trees as well as malfunctions and wearing out of the solar panels themselves. All these different factors are sources of variability in determining the effective solar potential available at the Mekelpark, and almost all will be taken into account while doing the solar potential calculations, generating a model of the expected kW per day for an area of the Mekelpark.

Research questions

Based on the literature study, several research questions were formulated;

1. What effect does the Sun's position have on solar potential?
2. How should building information be obtained?
3. How do the building characteristics effect the amount of sunlight hours?
4. How do weather conditions impact the solar potential?
5. How should a full map be obtained with the solar potential over the Mekelpark?

These questions will guide the investigation performed in this report. The potential of solar panels in the Mekelpark will be investigated in this Bachelor End Project report. Many links with the Bachelor program of Applied Earth Sciences can be found in this research paper. For example, as the energy market shifts from traditional fossil fuels to renewable resources, solar panels are an effective, cheap and universally applicable solution. A surprising link can also be found in the open pit mining field. Slopes and the locations light reaches from an import aspect of mine design and this report.

Prior to performing any calculations or measurements, an extensive literature study was performed, with the purpose to gather information on how other research studies with similar goals approached this topic. Most papers of these however, make use of complex point cloud data with advanced programming tools. For the purposes of this BEP report, it was decided to simplify the situation's geometry somewhat. However, these three reports, listed in the references (2, 3 & 4), proved significantly helpful as a guideline of the methodology of the subject of solar potential.

Chapter 2: Energy Potential of Solar Panels

In this chapter, first the earth's energy budget will be discussed and then the mechanics and workings of solar panels will be explained. The earth's energy budget is essential for determining the solar potential, since that is the energy that will be harvested by the solar panels. In the second section of this chapter the workings and mechanics of solar panels will be illuminated. An understanding of both the earth's energy budget and the workings of solar panels is vital for a better understanding to determine the solar potential. This gathered information will be used to answer the first research question: *What effect does the Sun's position have on solar potential?*

Chapter 2.1: Earth's Energy Budget

The sun emits an enormous amount of energy though the mechanism of nuclear fusion. In the sun's core, high pressure and temperature cause electrons to be stripped from hydrogen atoms. This frees the hydrogen nuclei to fuse together to form one helium atom. This is the basic process produces the sun's radiation energy, although the actual process is more complex.

This solar energy is short-wave radiation, which has wavelengths in the visible, near-ultraviolet and near-infrared spectra, with wavelengths between 0.1 and 5.0 µm. Short-wave radiation is classified differently from long-wave radiation, which contains less energy than short-wave. Long-wave radiation lies in the wavelength range from 4 to 40 µm[5]. The spectrum of wavelengths is visualized in figure 1.

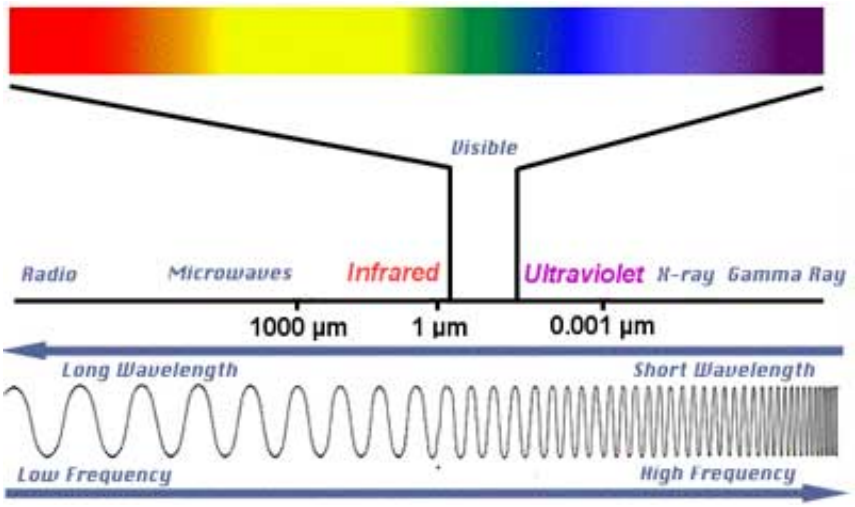

Figure 1: The range of the electromagnetic spectrum, from long wavelengths with low energy (radio) to short wavelengths with high energy (gamma rays) [6]

The sun contributes the largest portion of the earth's received energy. In theory, if all the energy emitted by the sun could be captured, 10 hectares would be enough to satisfy the entire world's demands in energy. Moreover, in a single hour the sun bathes the Earth in as much energy as the world consumes in an entire year.

However, three factors inhibit this energy harvesting. Firstly, the distance from the earth to the sun, which causes the sun's energy to be spread out, leaving only a section to hit the earth. This divergence of energy is illustrated in Figure 2. Secondly, the earth rotates about its polar axis, so only around half of the day, the sun's energy can be harvested. The third and most unpredictable factor is the atmosphere, a thin shell that surrounds the earth's surface. The atmosphere accounts for a 30% reduction in the sun's energy. Bad weather conditions can prevent almost entirely solar energy harvesting.[7]

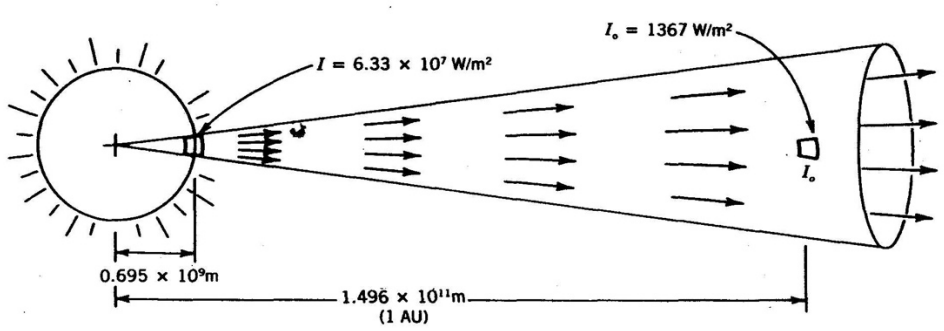

Figure 2: An illustration of the divergence of energy, due to the distance from the earth to the sun. This causes a spread of the sun's energy, which leaves only a section to hit the earth.[7]

The radiation intensity on the surface of the sun is around 6.33×10^7 W/m^2. The average earth-sun distance (1 AU) is around 1.496×10^{11} m. At this distance of 1 AU (roughly the mean distance from the Sun to Earth) the radiation intensity on the surface of the earth is around 1367 W/m^2 at the equator. The intensity of the solar radiation at a distance of 1 AU is called the solar constant I_{sc}.

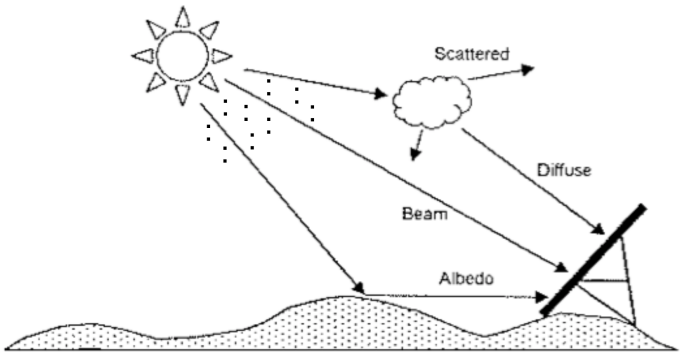

Figure 3: Whilst solar radiation travels to the Earth's surface it is effected by scattering, reflected and albedo. The aerosols are indicated with the dots in the atmosphere. [8]

Figure 3 illustrates how the solar radiation traveling towards a collector on the Earth's surface is affected by several mechanisms. The first 'filter' removes incident energy by scattering or absorbing by air molecules, clouds and other particles in the atmosphere. The scattered radiation which reaches the ground is called diffuse radiation, and the fraction that is reflected back into space is called albedo. The scope of the albedo depends on the Earth's surface. For example, oceans and rain forest reflect only a small portion of the sun's energy and thus have low albedos. Deserts, ice and clouds however reflect a large portion of the sun's energy and have a high albedo. On average about 30% of incoming solar energy is reflected back to space.

Radiation that reaches the surface directly and is not reflected or scattered is called beam radiation. Radiation that is reflected from the Earth's surface or ground onto the receiver is called albedo radiation. Adding all three of these components together is called global radiation. The standard solar irradiance value is accepted to be around 1 kW/m^2, although it varies significantly per location.

Chapter 2.2: Solar Panels

Several factors still contribute to the limited wide scale use of solar panels; immediate costs, dependability on weather conditions and design constraints. However, in the last 5 years many great leaps have been taken to tackle these problems. FlexSol is an example of one of these companies involved in solar panels.

These new developments in recent years have caused a dramatic drop in the cost of large-scale solar panels. Electricity from new large photovoltaic projects in 2013 was half as expensive on average as in 2010, bringing their costs much closer to the prices set by natural gas or other power plant options. The solar panel prices have been falling steadily for several years. These reductions are determined in large part by economies of scale as well as technological improvements and lower-priced panels manufactured in China.

Unlike fossils fuels, that still provide around around 80% of the world's power supply, solar panels (around 1% of the total energy world generation) generate electricity with no carbon pollution, no ashes or other waste production and with no other inputs other than sunlight. However, the manufacturing of solar panels does involve emissions.

Solar panels have been installed on a worldwide scale since the 1980's. The physical principles solar panels are based on, however, stem from the 19^{th} century and have not changed much since. In 1839 Edmond Becquerel, a French scientist, discovered that specific materials emitted

electric sparks when lit with sunlight. In the late 19th century, this property, called the photoelectric effect, was used in the first selenium photovoltaic (PV) cells.

The photoelectric effect is a phenomenon based on the principle that electromagnetic radiation is made of a series of photons. When a photon hits an electron on a metal surface, an electron can be emitted, which is called a photoelectron. In the left figure 4 the photoelectric effect is illustrated, here the red lines symbolize the light wave, hitting a metal surface. This causes (photo)electrons, indicated in blue, to be ejected from the metal.

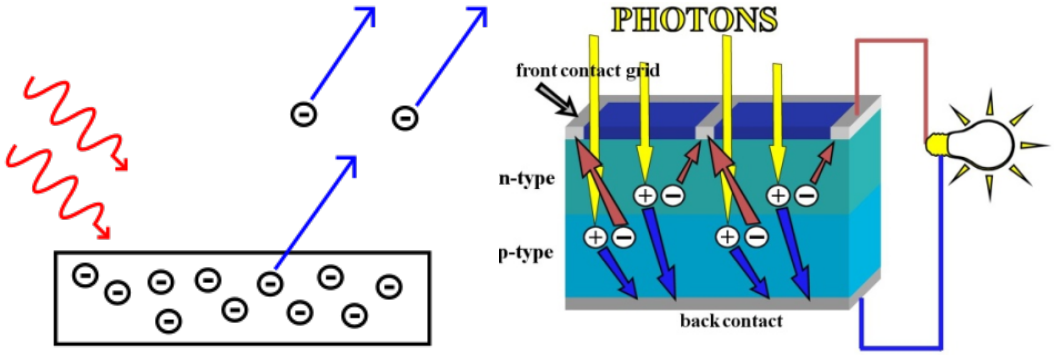

Figure 4: The right illustration shows the photoelectric effect, here the red lines symbolize the light wave, hitting a metal surface. This causes (photo)electrons, indicated in blue, to be ejected from the metal. The left illustration shows process in which the electrons are captured in the form on an electric current, which is then used as electricity. [9 & 10]

When the photon (in light energy) hits the metal surface, the photon's energy is absorbed by electrons in the metal, by knocking loose the atoms from the semiconducting material. If electrical conductors are connected to the positive and negative sides, they then form an electrical circuit. The electrons can be captured in the form of an electric current, which can be used as electricity. This is illustrated in the right figure 4.

If the light has a frequency below the minimum frequency (threshold frequency), no electrons will be ejected. This threshold frequency is a characteristic of the metal. The kinetic energy of the photoelectrons is also proportional to the light frequency. In the two graphs below, it can be seen that in Figure 5 (a) an increase in light amplitude will cause a linear increase the electron current and in Figure 5 (b) that the relationship between electron current and light frequency is constant, thus, the rate at which electrons were ejected from the metal remained constant as well.

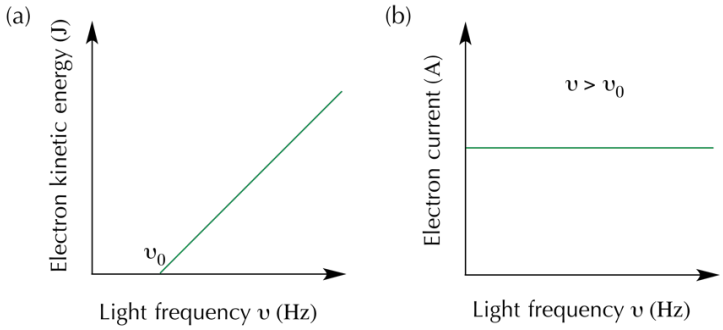

Figure 5: Two graphs, the first showing the electric kinetic energy plotted against the light frequency, showing their linear increase, the second showing the electron current plotted against the light frequency, showing that the relationship between electron current and light frequency is constant. [11]

The three most important factors that influence the amount of energy generated by the solar panels are:

- Location, since the amount of sunlight available will affect the amount of energy produced. Predictions of energy can be made for a certain location by use of statistical weather data.
- Tilt Angle, with the correct inclination towards the sun, the amount of light falling on the surface will increase, thus generating more energy. This angle of inclination depends upon the latitude of the proposed site. For example, solar panels on the equator will produce the maximum amount of energy when placed horizontally.
- Orientation of panels are also important factors in maximising energy production. On the Northern hemisphere a South oriented façade collects the most light throughout the year thus maximising energy production. Although East and Westward facing facades are not optima's in collecting light, they can still produce significant amounts of energy.

Combining these three factors will give you a good indication of the characteristics of the ideal solar panel placement. The data from MetData from Meteonorm for Amsterdam is given in table 1. This assumes a module efficiency of 13,5% and a performance ratio of 78%. The module efficiency determines the percentage of sunlight that hits your panel that is converted into usable electricity. The performance ratio describes the ratio between the actual and theoretical energy outputs of the PV plant, as a percentage.

Table 1	
Energy Output	129 kWh/m^2/y
Optimum Tilt Angle	40°
Orientation	62/5 (Latitude/Longitude)

Table 1: Solar Panel in Amsterdam Ideal situation

Solar irradiance is defined as the rate at which solar energy reaches a unit area on the earth, measured in watts per square meter (W/m^2). Solar irradiance is an immediate measurement of rate and varies over time. In solar panels the maximum solar irradiance is used to determine the peak rate of energy input into the system.

The solar radiation is also an important term for designing the solar panels. Solar radiation indicates how much solar energy has fallen on a collector over a period of time and is measured in watt-hours per square meter (Wh/m^2). Solar radiation can simply be determined by integrating the solar irradiance over the time period.

In Figure 6 a typical system of a photovoltaic cell is displayed, where the captured light energy from the sun is then used to drive an electric current. Unlike traditional electricity generation systems, which convert energy to heat or other forms of work, PV technologies convert the sun's radiant energy directly to electricity.

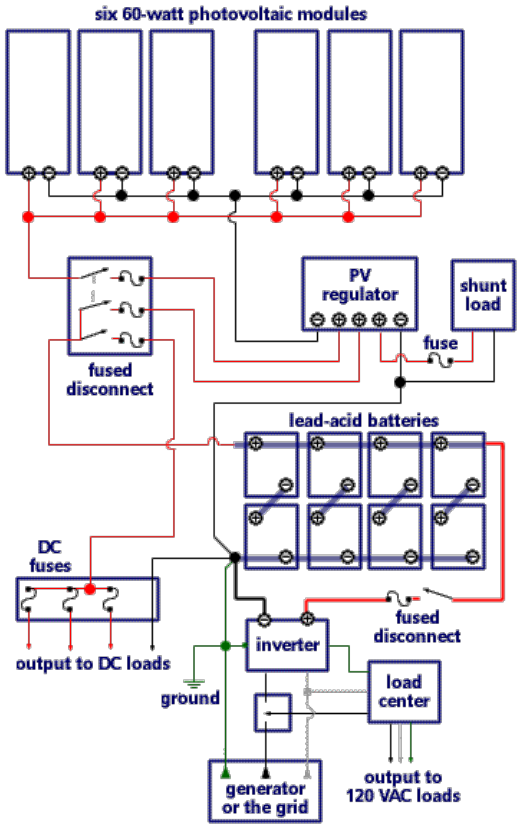

Figure 6: Typical system of a PV, where the captured light energy from the sun is then used to drive an electric current. [10]

The internal and external mechanism to make solar panels function are now understood, but the amount of sun at the investigated location is still unknown. This will be considered in the next chapter: Sun Duration for the Location.

Chapter 3: Solar Potential at a Certain Location

In this chapter the method for assessing the sun duration at the Mekelpark and subsequently the solar potential will be presented. First a description of the investigated site will be given, this is important for the determination of the geometry of the buildings. This data will be used to answer the second research question: *How should building information be obtained?* Next, the calculations of the sun position and their relevance will be presented and discussed, which answers the third research question: *How do the building characteristics effect the amount of sunlight hours?* Lastly, the addition of the weather factor will be considered, and it will be explained how to implement this effect into the calculations. Thus answering the forth research question: *How do weather conditions impact the solar potential?*

Chapter 3.1: Site Description

The Mekelpark is a park at the heart of the TU Delft Campus, which opened on the 5th June 2009. The investigated part of the park has an area of 250 by 160m, so 40.000 m^2 or 0.04 km^2 and has been visualized by a dotted line in figure 7. As can be seen in the image below, the most dominating features of our investigated area are the EWI building (on the right hand side of the figure) to the West, and the CiTG building (left hand side of the figure) to the East.

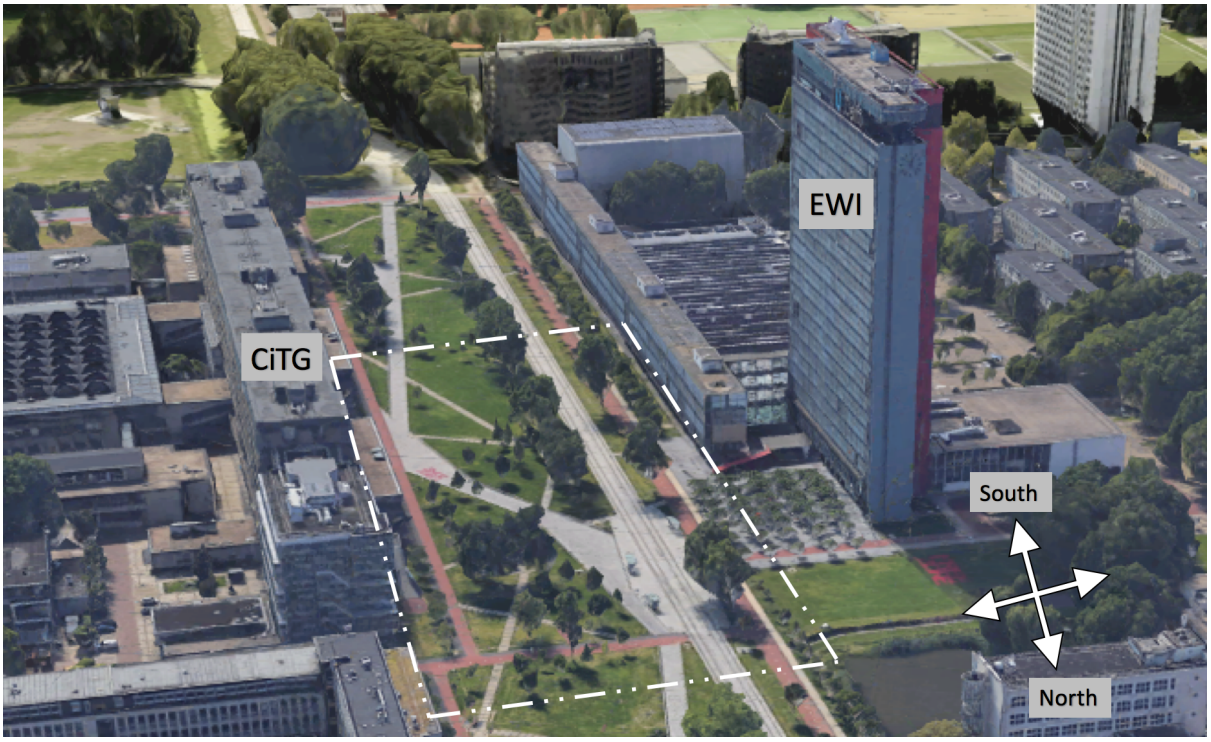

Figure 7: Image from Google Earth Pro

The geometry of these buildings is essential for determining the amount of sunlight hours per day and thus the solar potential, with the height of the buildings being the main factor. The Actueel Hoogte Bestand Nederland[11] (AHN), can help with this height step. AHN is elevation raster map for the entire Netherlands and contains detailed and precise height data with an average of 8 height measurements per square meter.

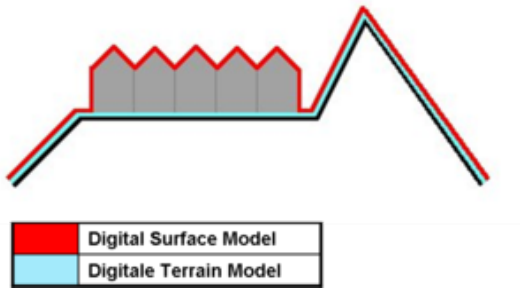

Figure 8: An illustration for the difference between the DSM and the DTM. For this paper the DSM is the data of interest. [12]

The PDOK[11] website offers a wide range of geo-information from the Dutch government, with among other things this AHN data. The 0,5 m raster dsm GeoTIFF file was downloaded. The dsm data is relevant for our purposes as opposed to the dtm data, because the dsm data contains services (buildings in other words), whilst the dtm data only contains the terrain information. This difference is illustrated in figure 8. Since we need the structures for an accurate shadow and light simulation, the dtm data is used. GeoTIFF is a public metadata standard allowing geo-referencing information to be embedded in a TIFF file (TIFF files are similar to JPEG files but are not compressed as JPEG files are, thus have a higher resolution). The AHN data was scanned in 2014. Tile 37en2 will be used for this project, since it contains our location of interest, the Mekelpark.

Below in Figure 9, the dsm data for Mekelpark is displayed. On the left side, shown in red and orange hues, is the EWI building and on the long building on the right is the CiTG building.

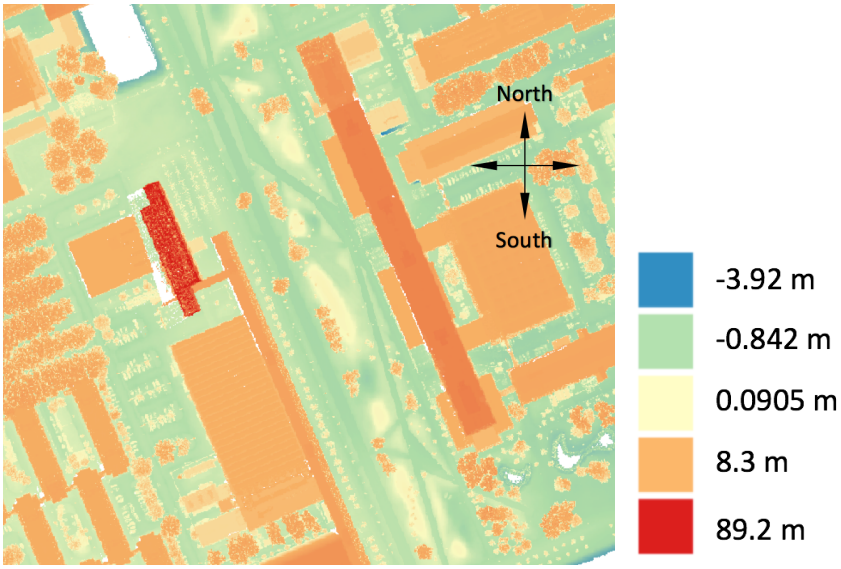

Figure 9: Dsm data for Mekelpark with 0,5 m raster, with on the right the EWI building and on the left the CiTG building.

Next, a profile was made across the Mekelpark using the Profile Tool in QGIS[13]. This was done to determine the height of both the CiTG and EWI building.

The profiles for 0,5 m are displayed in figure 10. Around the horizontal 100-meter mark some strange spikey data is found. This is strange since, as can be seen in the image at the start of this chapter, we expect the EWI building to be found here, which is flat on top. This could be due to the fact that the AHN data was unfiltered. Most likely, this data was gathered by a plane which monitored at an angle. For a tall building multiple height measurement will be taken at the same x and y coordinates. This is usually filtered out by taking the maximum value of these multiple heights for a single x and y coordinate. A form of manual filtering was performed for determining the height of EWI in figure 10.

The maximum height of 90 m for EWI was assumed for the purposes of this project. The slope was determined in figure 11 to corroborate the result. The CiTG building at the 300-meter horizontal mark, was found to be 33 m. This building does not exhibit the same strange behaviour of the EWI building, which backs up the assumption about the unfiltered data height of EWI being the problem, due to it's significant height. Around the 200-meter mark trees and other obstacles in the Mekelpark can be found. Since the lampposts are around 2.5 m height, most of this relief doesn't impact our results so it's effect will be neglected in this report, however in the discussion the effect will be explored further.

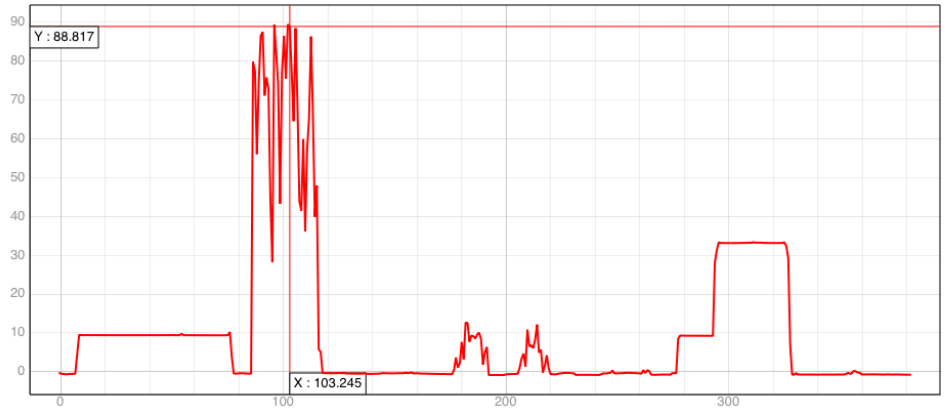

Figure 10: Elevation Profile with Dsm data from West to East

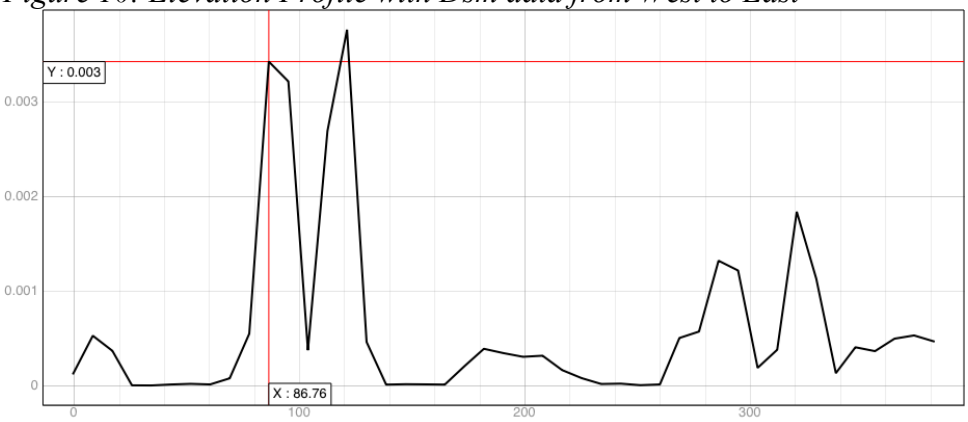

Figure 11: Slope profile with Dsm data from West to East

For simplification purposes in the model, it was decided to focus solely on the shadow effect of these two buildings. This simplified situation is illustrated in figure 12.

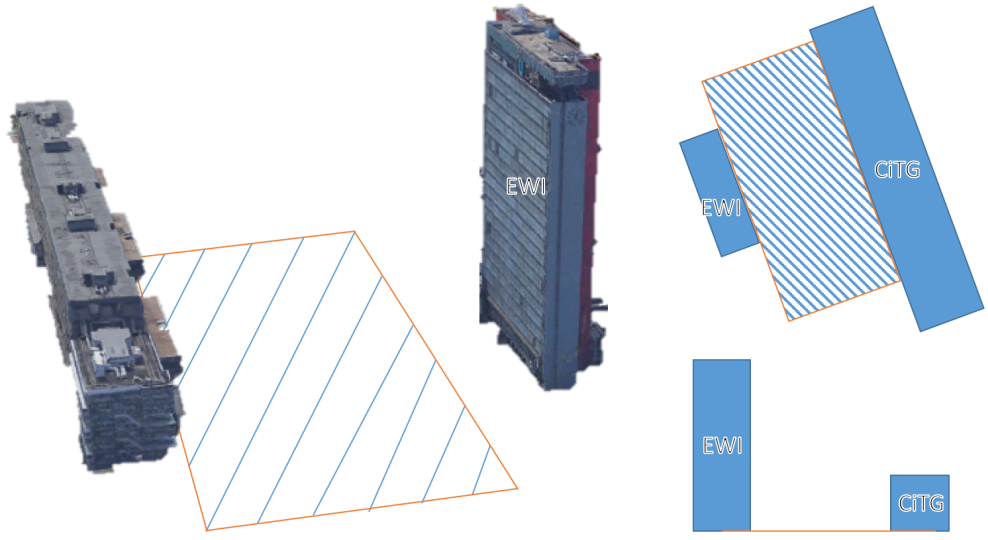

Figure 12: Simplified geometry of the Mekelpark, used for the subsequent calculations in chapter 3.

Chapter 3.2: Sunlight Geometry Calculations

Introduction

The goal of this chapter is to determine the amount of time shadows are casted at certain locations of the Mekelpark, purely due to the geometry of the EWI and CiTG building. The heights and locations of both of these were determined in the previous chapter. As the sun moves across the sky, the shadows cast will alter the amount of light that can potentially be captured by the solar panels. To establish this amount of time, first the 'required' elevation angle needed for each azimuth is calculated, and then the sun's position throughout 24 hours of 365 days of the year was generated.

Background Theory

Using the University of Oregon's Sun Path Chart Program[14], figures 13 & 14 were obtained. A sun path charts plots the sun's elevation angle and azimuth angle over a day, at a certain location. In figures 13 & 14 the coordinates specified were a latitude of 51.99° and a longitude of 4.37°, which is in the middle of the Mekelpark and thus relevant for this report.

These sun charts can be plotted in Cartesian coordinates. With Cartesian coordinates the solar elevation is plotted on one axis and the azimuth on the other. In this program the latitude and longitude are entered and certain specifications for the data, such as the time zone and the dates to be plotted. In figure 14, the Cartesian coordinates plot shows dates 30 or 31 days apart, between solstices, December through June with the solar elevation on the y-axis and solar azimuth on the x-axis. This solstice occurs twice a year, when the Sun reaches its most northerly or southerly point relative to the equator. Figure 15, shows this data form June to December. These are plotted separately for clarification purposes. The figures provide a lot of information on the Sun's position. For example, on the date of March 16th (blue parabolic lines show dates) at 12 o'clock (red vertical lines show hour of day) the solar elevation is 35° and solar azimuth is 165°. This situation is illustrated in figure 13.

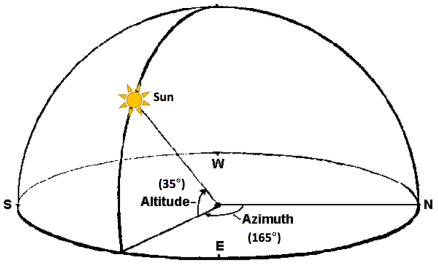

Figure 13: Clarification of the situation on March the 16th were the solar elevation is 35° and the solar azimuth is 165°.

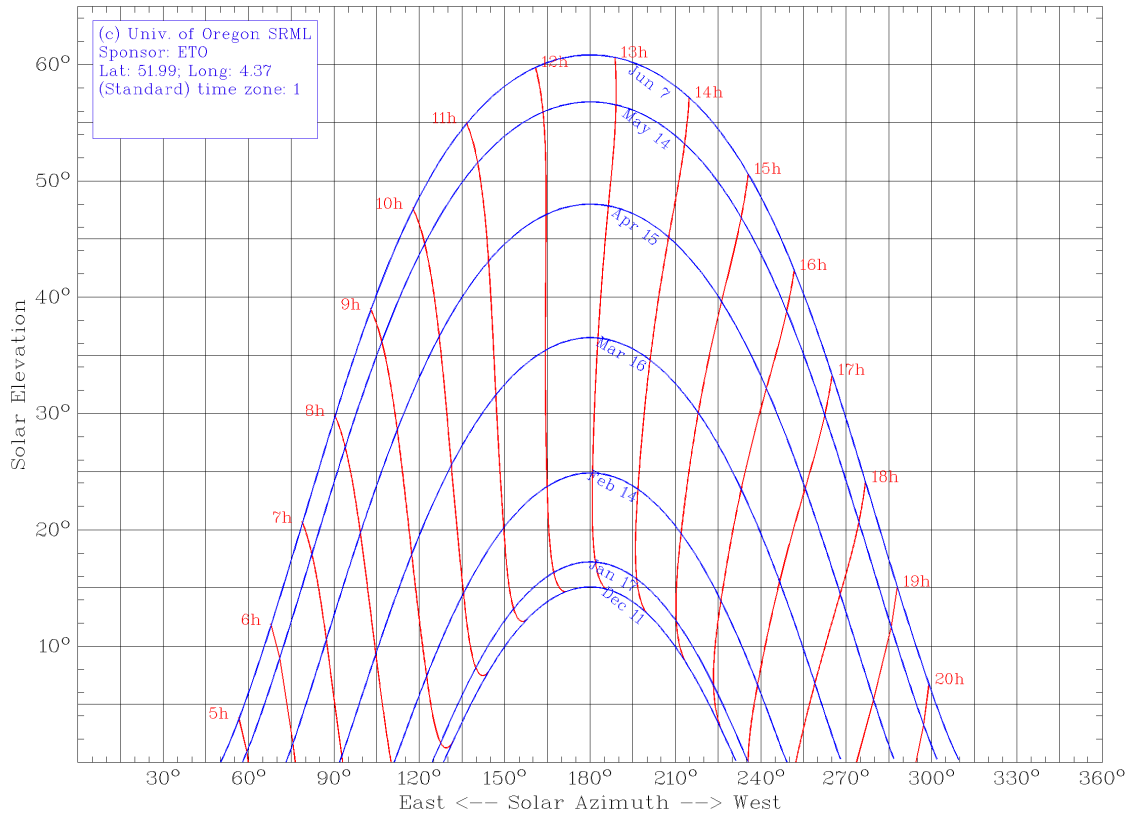

Figure 14: Cartesian Coordinate Sun Path Chart Program at Latitude: 51.99 and Longitude: 4.37. Plot dates having average solar radiation for December through June

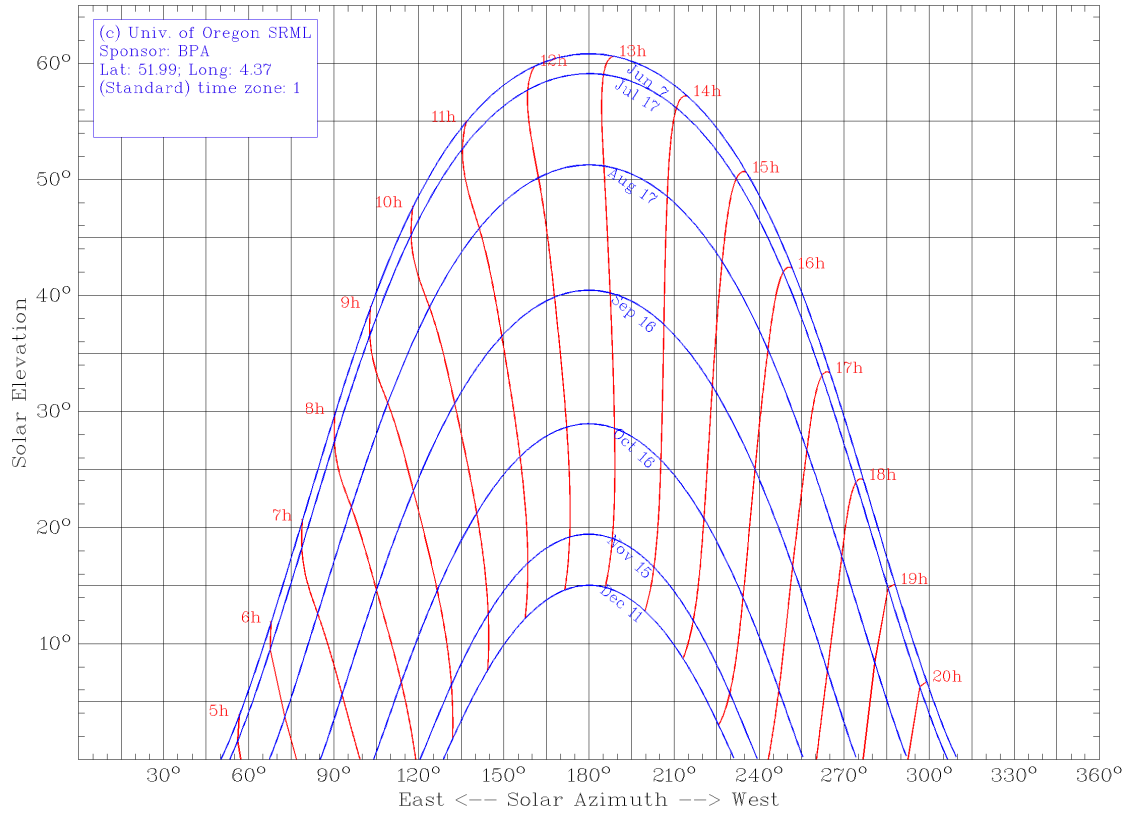

Figure 15: Cartesian Coordinate Sun Path Chart Program at Latitude: 51.99 and Longitude: 4.37. Plot dates having average solar radiation for June through December

The solar azimuth angle describes the direction of the Sun, while the solar elevation angle describes how high the Sun is. The solar elevation is the altitude of the Sun, which is the angle between the horizon and the centre of the Sun's disc. The solar azimuth is a method for describing an angle in a spherical coordinate system. It describes the angle made between a reference direction (for example North in figure 16) and a line on the reference plane from the observer to a point of interest. Both the solar elevation and solar azimuth are illustrated in figure 16.

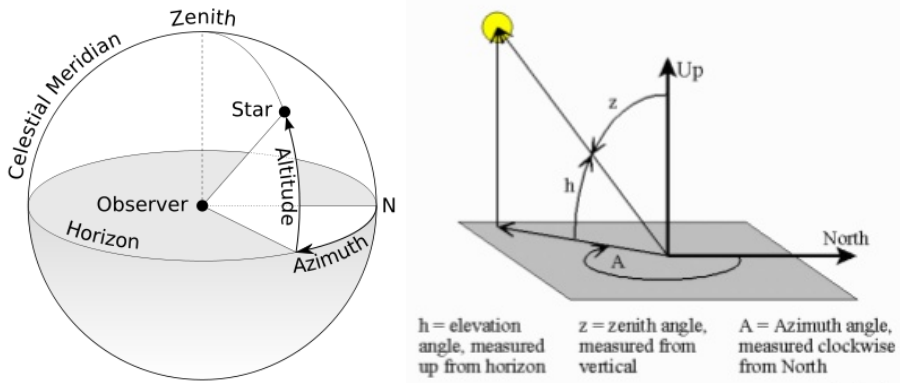

Figure 16: Definitions of solar elevation and solar azimuth[15 & 16]

The azimuth (denoted as α) is calculated by the formula below:

$$\tan \alpha = \frac{\sin L}{\cos \varphi_1 \tan \varphi_2 - \sin \varphi_1 \cos L}$$

where the latitude φ_1 is the observers latitude with longitude zero. The point of interest has latitude φ_2 and longitude L (positive eastward). In this formula we approximate the earth as an exact sphere.

The solar elevation angle is calculated with the following formula:

$$\sin \alpha_s = \sin \phi \sin \delta + \cos \phi \cos \delta \cos h$$

where α_s is the solar elevation angle, h is the hour angle (in local solar time) and δ is the current declination of the Sun and ϕ is the local latitude. The hour angle is one of the coordinates used in the equatorial coordinate system to give the direction of a point on the celestial sphere. Declination's angle is measured North or South of the celestial equator, along the hour circle passing through the point in question. The hour angle and declination are the two angles that locate a point on the celestial sphere in the equatorial coordinate system, the other being hour angle.

Programs Used

Several programs were used for calculating the sunlight geometry. The first program used for the elevation data was QGIS. It is an open source and free Geographic Information System. It is an effective tool for visualization, editing and analysis of data.

The primary program used was Matlab, which is a multi-paradigm mathematical computing environment. It allows for creation and manipulations of matrices, plotting and interpolation of data and functions.

Data Used

In figure 17 a slice perpendicular to the two buildings is shown. The α and β indicate the solar elevation of the Sun. In the most simplified situation, if the solar elevation necessary to cast a shadow on point X is calculated between the two buildings, this could be used to calculate the percentage of time point X is receiving direct sunlight.

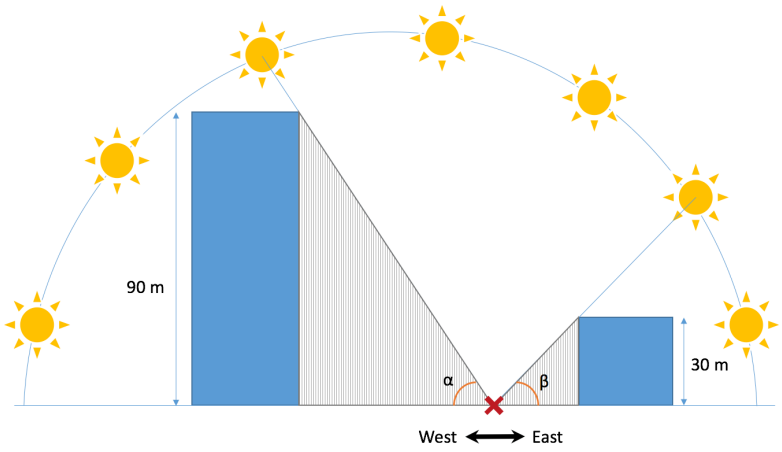

Figure 17: Simple situation for calculating the necessary solar elevation

However, the position of the Sun throughout the year is more complex than the situation presented above. In reality the Sun takes a different route across our sky every year, if viewed from the earth's surface. The Sun rises earlier every day until the June 21st, then starts rising later. It also climbs higher in the summer, and doesn't rise exactly due east. Thus the Sun's point in the sky is at a different time each day. There are two main factors contributing to these anomalies; the Earth is tilted on its axis 23.5° in relation to the plane of its orbit around the Sun and The Earth does not orbit the Sun in a circle, but in an ellipse. In figure 18, a comparison can be made between the situation in the middle of June and in the middle of December.

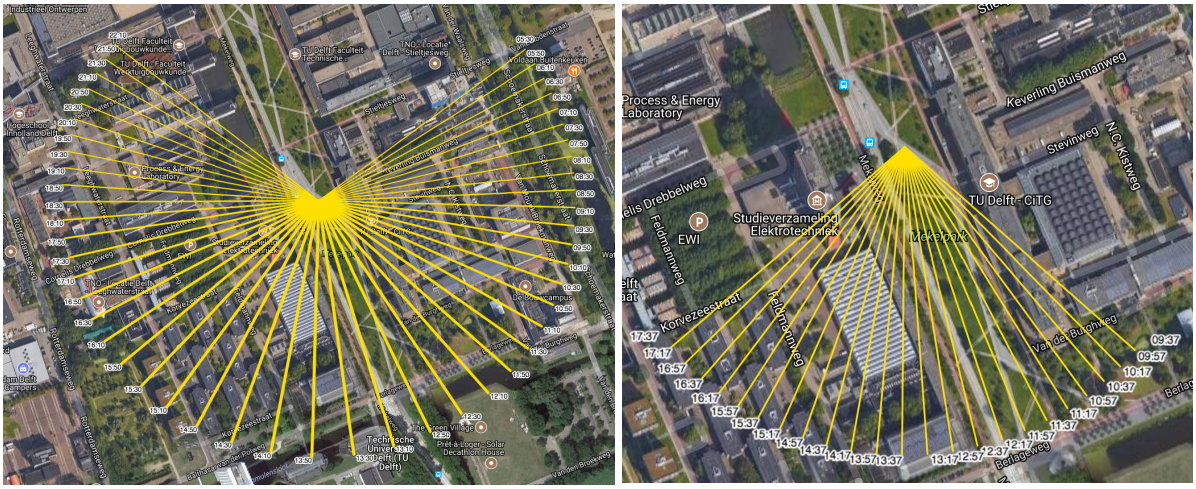

Figure 18: Comparison of the Sun position in mid-summer and in mid-winter, the yellow lines indicate the time of day. The 'scope' of the Sun is clearly different for both times of year.[17]

Since the triangle on which the calculations will be performed is a scalene triangle (displayed below), the Law of sine's will be used (also displayed below).

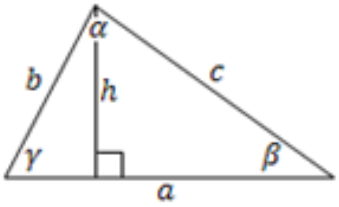

$$\frac{a}{\sin\alpha} = \frac{b}{\sin\beta} = \frac{c}{\sin\gamma}$$

Now that the distance between the point and the building has been found, the necessary Sun elevation can be calculated. It was chosen to calculate the azimuth every 1° degree, ultimately calculating it for all 360° with a Matlab code. In figure 19, a Google Earth satellite image is displayed next to a schematic image of the investigated situation for a single location.

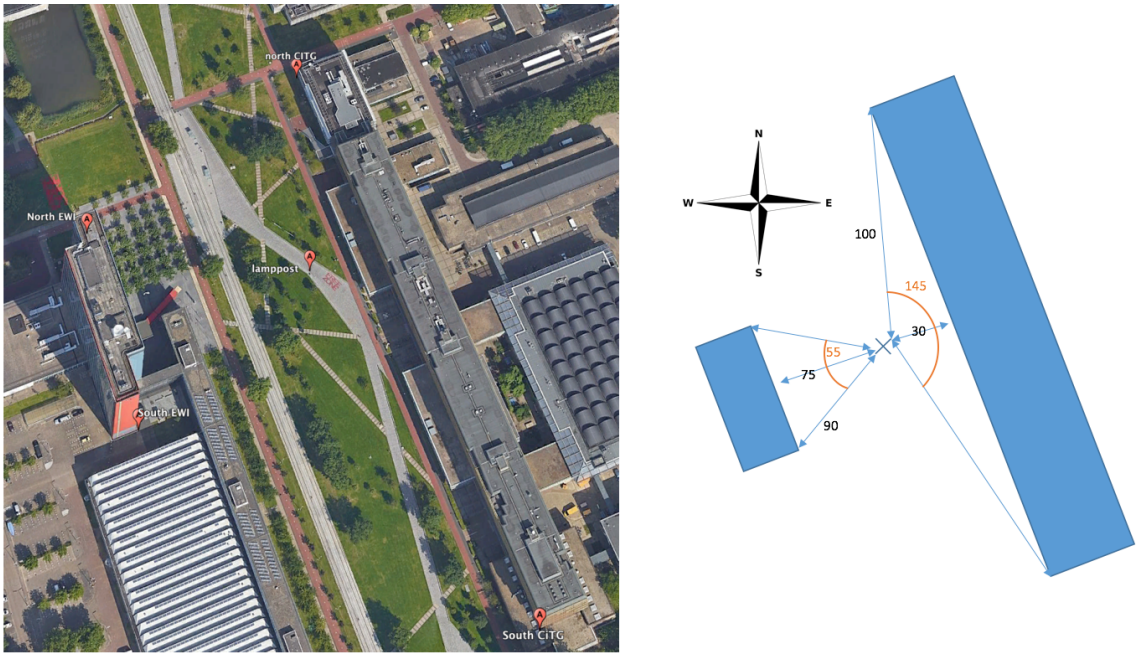

Figure 19: To the right a Google Earth satellite image of the Mekelpark & to the left a schematic image of the investigated situation for a single location, with the corresponding angles and distances.

The approach for the coding was to determine the necessary Sun altitude for each azimuth, then to code the Sun's altitude throughout the year, each hour. After which the amount of time the minimum Sun altitude was reached throughout the year could be determined as a percentage.

The Matlab code written for the necessary Sun altitude for each azimuth can be viewed in the Appendix A.1 and a plot can be found in figure 20. This figure illustrates that, for example, the required elevation for EWI (around 65°) is much higher than the elevation for CiTG (around 30°).

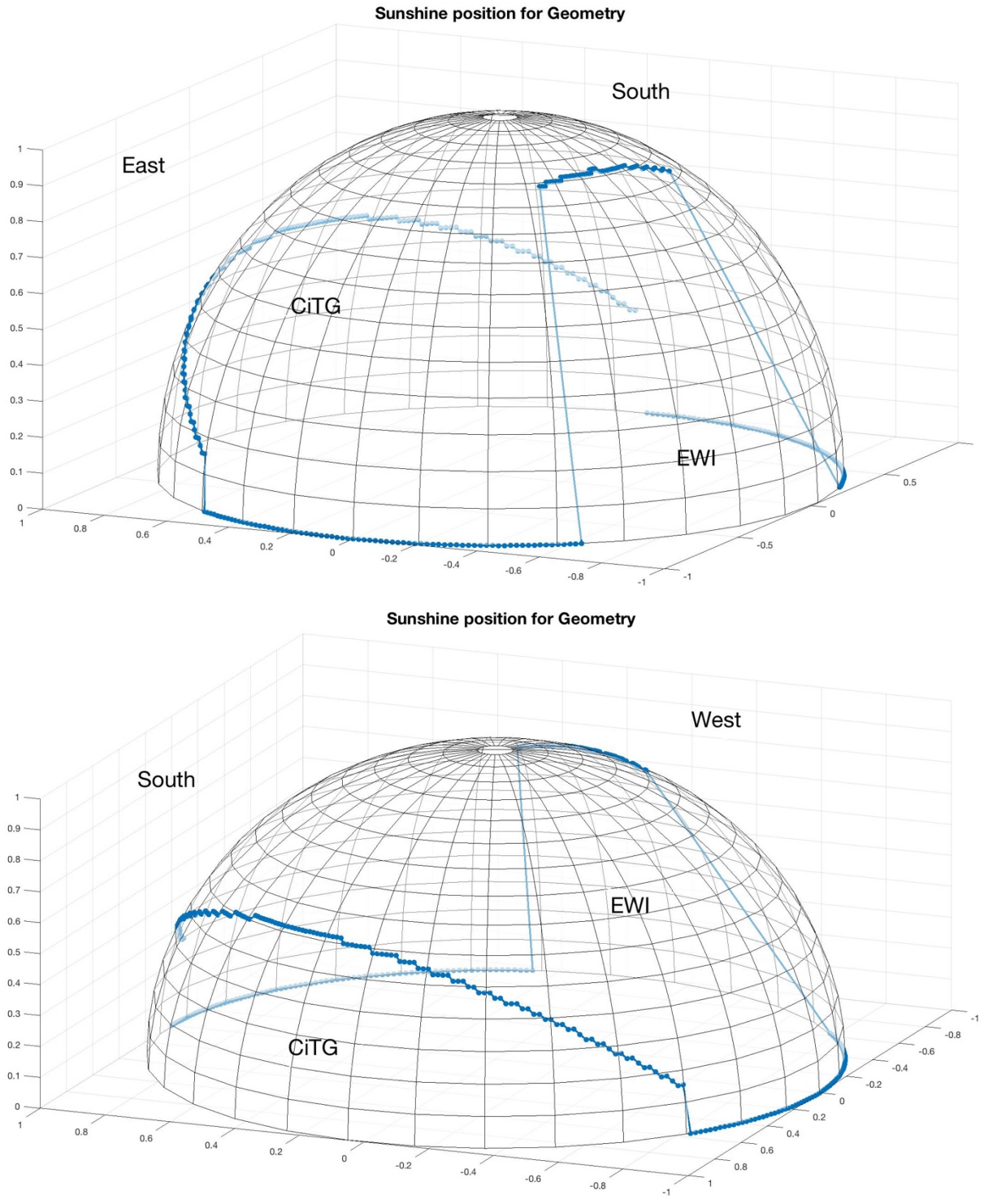

Figure 20: The necessary Sun altitude for each azimuth

Then a Matlab code was necessary to plot the Sun's position throughout the year for every hour. This was done using the NOAA Solar Calculator[17] and Astronomical Algorithms by Jean Meeus (1991). The input arguments are; latitude and longitude of the location, the time zone and the specific hour and day. This code was altered in Matlab to calculate the Sun position for

every hour and every day for an entire year. Then a hemisphere was graphed in Matlab, for a visualization of the Sun's position throughout time. The code itself can also be found in the Appendix A.1. Below all formula's used to calculate the Sun's position over the year are explained.

$$Julianday\ (JD) = date + 2415018.5 + time - \left(\frac{timezone}{24}\right)$$

$$Juliancentury\ (JC) = \frac{JD - 2451545}{36525}$$

Julian Day is an integer defined as an entire solar day, with Julian day 0 being January 1, 4713 BC. The 31st of October 2017 in this unit is 2458057. Using this unit simplifies calculations compared to the Julian Calendar. This is linked to the Julian Century, which is a unit of time which equals exactly 365.25 days. From the starting data of Julian day 0 to 2000 AD there are 6712 years. Since years have 365.25 days, this corresponds to 6712*365.25=2451558. Since the Gregorian calendar is 13 days ahead of the Julian calendar, the value of 2451545 arises in the formula.

$$Geometric\ Mean\ Long\ Sun\ (GMLS) = mod(280.46646 + (JC * 3600.76983) + ((JC^2 * 0.0003032, 360)$$

$$Geometric\ Mean\ Anom\ Sun\ (GMAS) = 357.52911 + (JC * 35999.05029) - (0.0001537 * JC^2)$$

$$Eccent\ earth\ Orbit = 0.016708634 - (JC * 0.000042037) + (0.0000001267 * JC^2)$$

$$Sun\ Eq\ of\ Ctr\ (SEC) = sin(GMAS) * (1.914602 - JC * (0.004817 + 0.000014.* JC)) + sin((2 * GMAS)) * (0.019993 - 0.000101.* JC) + sin((3 * GMAS)) * 0.000289$$

$$Sun\ True\ Long\ (STL) = GMLS + SEC$$

$$Sun\ App\ Long\ (SAL) = STL - 0.00569 - 0.00478 * sin(125.04 - 1934.136 * JC)$$

The six formulas above account for the orbital eccentricity of the Sun. The eccentricity determines the amount by which the orbit of the earth around the Sun deviates from a circle. This value can range from 0 to 1. If the orbit is perfectly circular the value is zero, and as it becomes more elliptical it increases towards one. The eccentricity of the earth's orbit around the Sun is illustrated in figure 21. What is also visible in figure 21, is that during the Northern winter/Southern summer season, the distance between the earth and Sun is shorter than the distance during the Northern summer/Southern winter. This is effect is also taken into account in these six formulas.

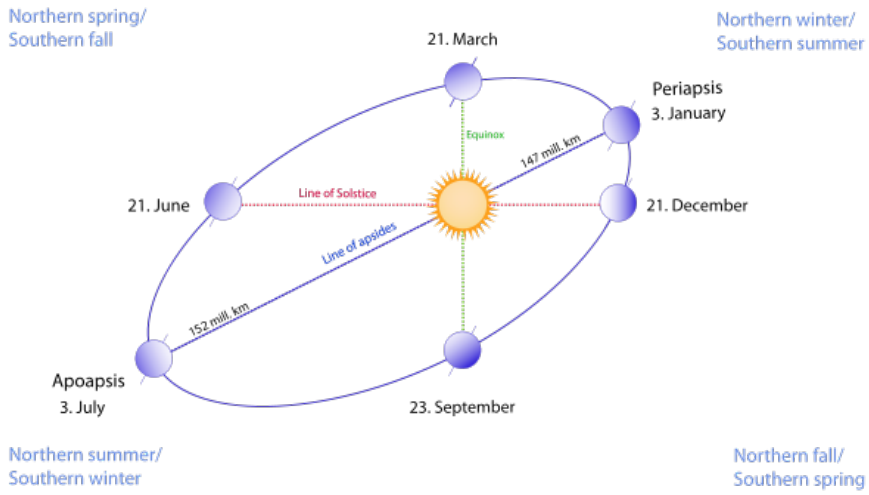

Figure 21: The eccentricity of the earth's orbit around the Sun, used in the calculations for the Sun position. [18]

$$Mean\ Obliq\ Ecliptic\ (MOE) = 23 + \frac{(26 + (21.448 - JC * (46.815 + JC * (0.00059 - JC * 0.001813)))}{60^2}$$

$$Obliq\ Corr\ (OC) = MOE + 0.00256 * cos(125.04 - 1934.136 * JC)$$

In the two formula above a correction must be made to take the Sun's axial tilt or obliquity into account. The axial tilt is the angle between the rotational axis and the orbital axis. This angle is illustrated in figure 22: The Earth's axial tilt is around 23.5°

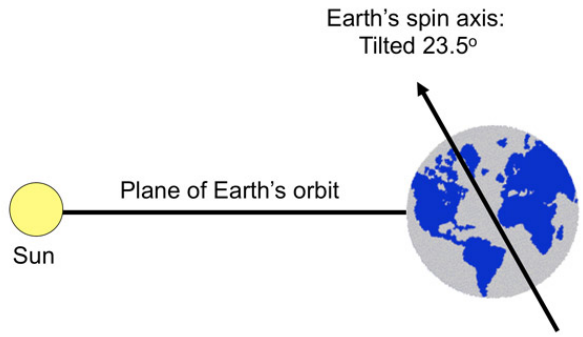

Figure 22: Earth's axial tilt is around 23.4°, used in the calculations for the Sun position [19]

$$Sun\ Decline\ (SD) = asin\ (sin(OC) * sin(SAL\ ))$$

$$var_y\ (Vy) = tan^2\left(\frac{OC}{2}\right)$$

$$Eq.of\ Time\ (ET) = \left(var_y * sin(2 *\ GMAS)\right) - \left(2 * var_y * sin(GMAS)\right) + \left(4 * MOE * var_y * sin(GMAS) * cos(2 * GMAS)\right) - (0.5 * Vr^2 * sin(4 * GMAS))$$

The equation of time defines the difference between the two kinds of solar time; the apparent solar time and the mean solar time. The apparent solar time tracks the diurnal (daily) motion of the Sun, whilst the mean solar time tracks a theoretical mean Sun with noon's 24 hours apart.

$$True\ Solar\ Time\ (TST) = mod(hour\ of\ day * 1440 + ET + 4 * longitude - 60 * timezone, 1440)$$

$$if\ \frac{TST}{4} < 0, Hour\ Angle\ (HA) = \frac{TST}{4} + 180$$

$$if\ \frac{TST}{4} > 0, Hour\ Angle\ (HA) = \frac{TST}{4} - 180$$

The hour angle is a coordinate used in the equatorial coordinate system to indicate the direction of a point on a celestial sphere. The hour angle of a point is the angle between the plane of the

Earth's axis and the zenith (meridian plane) and the plane of the Earth's axis and the point.

$$Solar\ Zenith\ Angle\ (SZA) = acos(sin(latitude) * sin(SD) + (cos(latitude) * cos(SD) * cos(HA)))$$

$$Solar\ Elevation\ Angle\ (SEA) = 90 - SZA$$

$$if\ Hour\ Angle > 0$$

$$Solar\ Azimuth\ Angle\ (SAA) = \frac{acos\ (sin(latitude) * cos(SZA)) - sin\ (SD)}{cos(latitude) * sin\ (SZA)} + 180$$

$$if\ Hour\ Angle < 0$$

$$Solar\ Azimuth\ Angle = mod(540 - \frac{acos(sin(latitude) * cos(SZA)) - sin(SD)}{cos(latitude) * sin(SZA)}, 360)$$

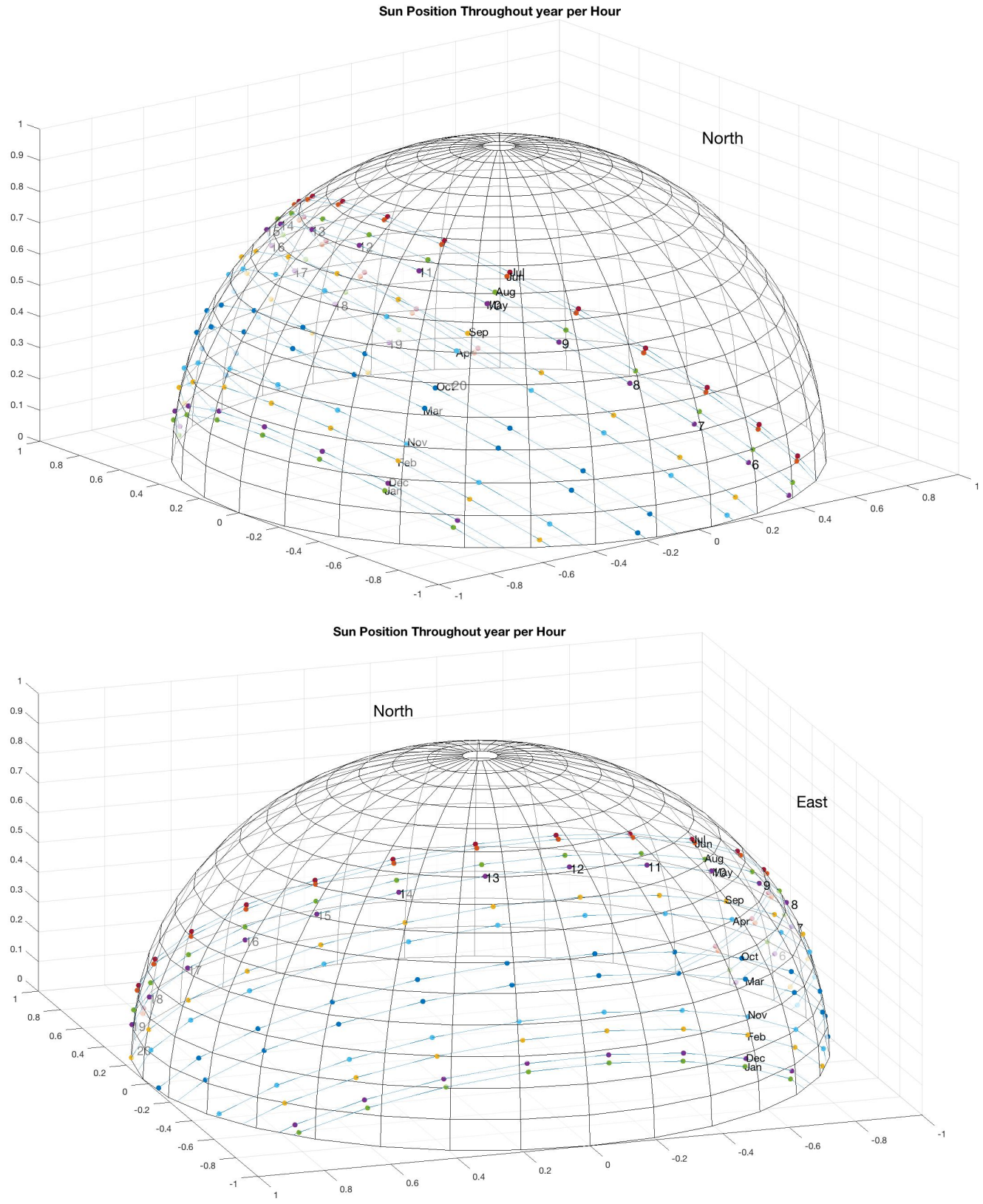

Figure 23: Results of the Sun position calculations. The first day of the month has been plotted for all 24 hours..

Here several angles are shown of the generated Sun path on a sphere using the code described

above for the first day of the month. North and East are indicated in these images, as well as the month and the hour of day. As is to be expected the Sun rises in the east and throughout the day moves to the west, were it eventually sets.

Now the necessary/required azimuth and elevation and the Sun position throughout the day over the entire year. By reconstructing the matrices and setting the required azimuth and elevation as a condition to be met by the calculated Sun position, a 24 by 365 matrix is created for every cell if the Sun position is met by the required conditions, the cell is changed to a one. This is then surmised per day, to generate the amount of hours per day that the necessary azimuth and elevation are met. The Matlab code can be found in the appendix.

Since a vector of the amount of hours of sunlight per day has been achieved, a simple summation will create the amount of hours of sunlight over an entire year. If this process is repeated over a number of points, an interpolation can be made, using the curve-fitting tool in Matlab. For example, for point 6 (see Chapter 4.1), it was concluded that in one year 2262 hour of direct sunlight hits that location. Since there are 8760 hours in a year, it can be concluded that 25,82% of the year there is direct sunlight at a considered location in the centre of the Mekelpark.

Chapter 3.3: Addition of Weather Factor

Introduction

Figure 24 illustrates the earth's energy budget, which is the balance between the Sun's incoming energy with the outgoing (thermal) long-wave and the reflected shortwave energy from the Earth. The fraction of this relevant to our studies is the 51% absorbed by land and oceans[21]. This solar energy reaching the Earth's surface is quantified as the solar constant, the annual average solar flux per unit area normal to the flow direction (or the irradiance) received outside the Earth's atmosphere. This is estimated to be around 1370 W/m^2 according to figure 24. This varies throughout the year due to the characteristics of the Earth's orbit about the Sun. At different heights, in different components of the atmosphere, the range of absorption and scattering differs. The reduction of the solar input from clouds in the

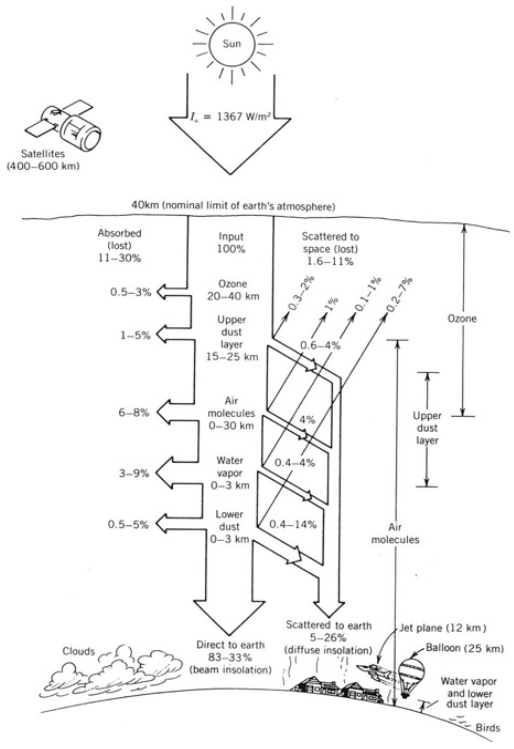

Figure 24: earth's energy budget [21]

atmosphere can range from 30% on a very clear day to almost 90% on a very cloudy day.

Background

On the KNMI website[22] monthly overviews of the weather in the Netherlands are published. This data is taken from Dutch meteorological stations. From these tables the sunshine duration (in hours and in percentages) and radiation (J/cm^2) was determined for the Delft area. An example of the data in the monthly overviews is displayed below.[23]

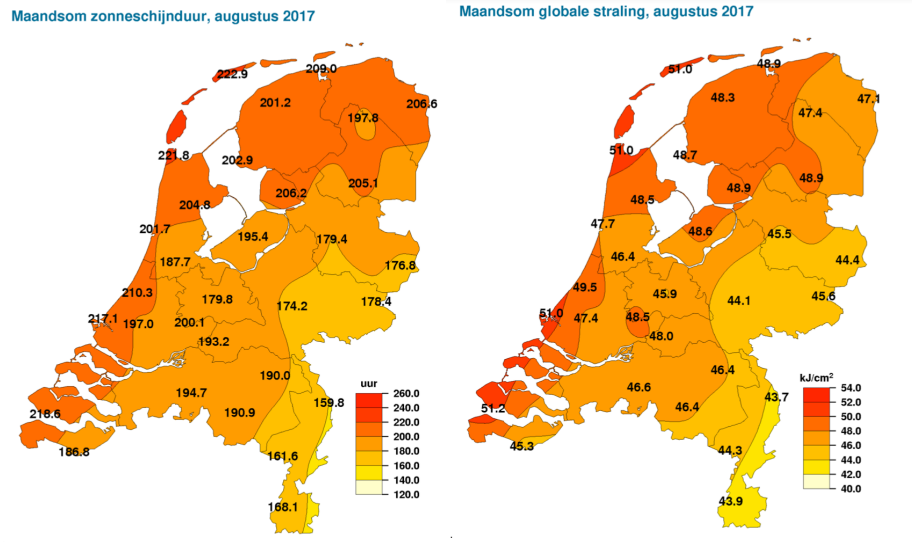

Radiation (J/cm^2), as defined by the KNMI, is the summation of the direct and diffuse Sun radiation and is measured at a point where the sunbeams are uninhibited the entire day. The basis of the calculations is a 10-minute sum of energy of Sun and sky radiation which has been converted into warmth on a horizontal surface. The radiation is dependent upon the Sun height, the canopy cover and the type of cloud coverage. [24]

These measurements are performed with a pyranometer, an image of which can be found in figure 25. A pyranometer measures irradiance, the total amount of radiant energy on a flat surface. A tracker inside the pyranometer follows the Sun to make sure the beam is directed into the device. A pyranometer contains a thermophile detector, a device that converts thermal energy into electrical energy. This detector is covered with a strongly light-absorbing black paint such that it consumes all radiation from the Sun equally. The temperature difference created between black surface of the sensor and the instrument's body results in a small voltage at the sensor that is converted into W/m^2.

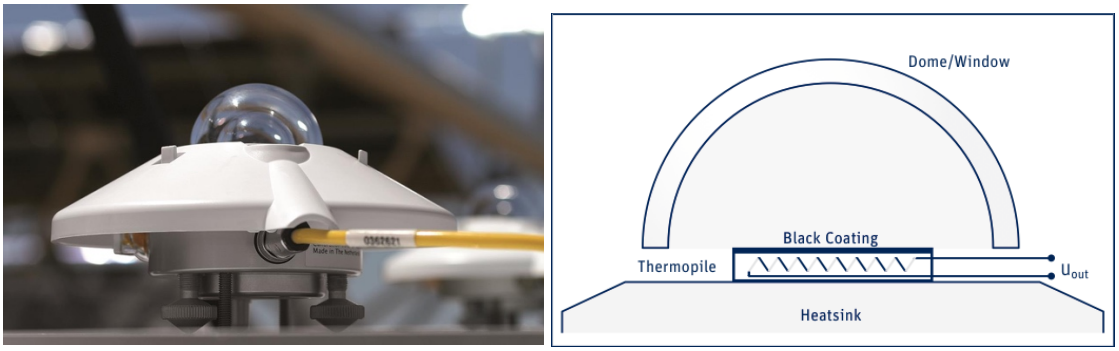

Figure 25: a pyranometer in the field & a schematic drawing of the instrument

Sunshine duration is measured hourly based on 10-minute data of the radiation. The maximum sunshine duration is the timeframe between sunrise and sunset. The percentage sunshine indicates how much the Sun shines in comparison to that maximum. A day is deemed 'sunless' if all 10-miniute values fall below a certain threshold point.[24]

Data

From the KNMI website monthly overviews of sunshine duration (in hours and in percentages) and radiation (J/cm^2) were determined for the Delft area. This data spanned a duration of 8 years (2009 to 2017). This full data can be found in the Appendix A.2. The mean, median and standard deviation were determined from this data for each month. Converting radiation in J/cm^2 to W*h/cm^2, and assuming an area of 200 cm^2 solar panel per lamppost, the Watts hour can be determined. Multiplying the Watts hour (the amount of Watts generated in one hour) by the hours of sunlight for each area of the Mekelpark for each month, the solar potential per month of the Mekelpark can be determined. The Matlab code for this computation can be found in the Appendix A.1.

Mean of data from KNMI-data, full data in Appendix B			
Mean	Sunshine Duration (hours)	Percentage (%)	Radiation (J/cm^2)
Jan	71,9	27,9	7831
Feb	84,2	30,0	12677
Mar	163,5	44,3	29729
Apr	210,4	50,4	45928
May	222,7	45,9	56008
Jun	217,2	43,6	58105
Jul	221,5	44,1	57807
Aug	209,9	46,1	50703
Sep	167,1	44,0	33722

Oct	121,4	36,8	19453
Nov	69,0	26,0	8720
Dec	60,4	25,1	5943

Median of data from KNMI-data, full data in Appendix B			
Median	Sunshine Duration (hours)	Percentage (%)	Radiation (J/cm^2)
Jan	68,7	27,0	7572
Feb	81,6	29,0	12547
Mar	157,8	43,0	28477
Apr	200,4	48,0	45236
May	222,4	46,0	57000
Jun	226,8	46,0	59926
Jul	223,6	45,0	57173
Aug	219,0	48,0	51011
Sep	161,3	42,5	33039
Oct	116,2	35,5	19281
Nov	63,9	24,0	8510
Dec	55,6	23,0	5923

Standard deviation of data from KNMI-data, full data in Appendix B			
St. Dev	Sunshine Duration (hours)	Percentage (%)	Radiation (J/cm^2)
Jan	10,9	4,3	606,9
Feb	22,5	7,7	1904,8
Mar	22,7	6,3	2299,1
Apr	33,9	8,2	3995,8
May	24,4	5,0	3747,6
Jun	32,8	6,4	4960,4
Jul	28,2	5,8	4134,2
Aug	29,9	6,6	5900,4
Sep	22,1	5,8	2506,3
Oct	13,9	4,1	1056,6
Nov	16,5	6,3	955,6
Dec	12,4	5,1	612,2

After determining the solar potential (in kW) for the selected 24 points, an interpolation will be performed to create a map over the entire area. This interpolation was performed with the curve-fitting tool in Matlab. This tool allows the use of various interpolation methods, Nearest Neighbour, Linear and Cubic.

Nearest Neighbour interpolation[26] keeps the input values exactly the same and determines the value of the output cell by the nearest cell in the grid. It can be used on continuous data but the results will be blocky.

Linear interpolation uses a weighted average of the four nearest cell centres. The shorter the distance between the input cell and the output cell, the higher the weight (or influence) of (or on) the input cell.

Cubic interpolation looks at the nearest 16 cells from the output cell and fits a smooth curve through these points to find the value. This has an influence on the input values but can also cause the output value to be outside the range of the input values (which would show up as peaks or drops in the data). These various methods of interpolation are illustrated in figure 26.

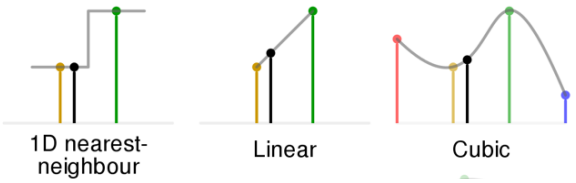

Figure 26: Illustrations various interpolation methods; Nearest Neighbour, Linear and Cubic.[27]

Chapter 4

In this chapter the results of calculations of the sunlight hours and the subsequent calculations for the radiation in kW over the investigated area in the Mekelpark, are presented. Next total amount of kW produced over the entire year is estimated, this will be converted into an amount of time the streetlamps can run fully on the generated solar panel power. Summarising this chapter will answer the last research question: *How should a full map be obtained with the solar potential over the Mekelpark?*

Chapter 4.1: Results Light & Geometry

After determining the solar potential (in kW) for the selected 24 points, an interpolation will be performed to create a map over the entire area. This interpolation was performed with the curve-fitting tool in Matlab. This raster pattern consists of 24 points, evenly distributed over the area. Using their coordinates and their geometric relationship with the surrounding buildings, the amount of hours' sunlight hits the location directly was calculated for all 24 points. Using the curve fitting tool in Matlab, an interpolation over the area was performed, generating a 'heat map' of the sunlight hours. The curve fitting tool allows interpolation using various methods; Least-squares, cubic and linear. The three maps using these methods can be found in figures 27 through 29.

On the top of EWI a purple colour marker is indicated, which serves as a reference. This marker indicates 4453 hours, which is the amount of sunlight hours when both building's (CiTG and EWI) effects are neglected in the calculations. So this is the situation where there are no shadows.

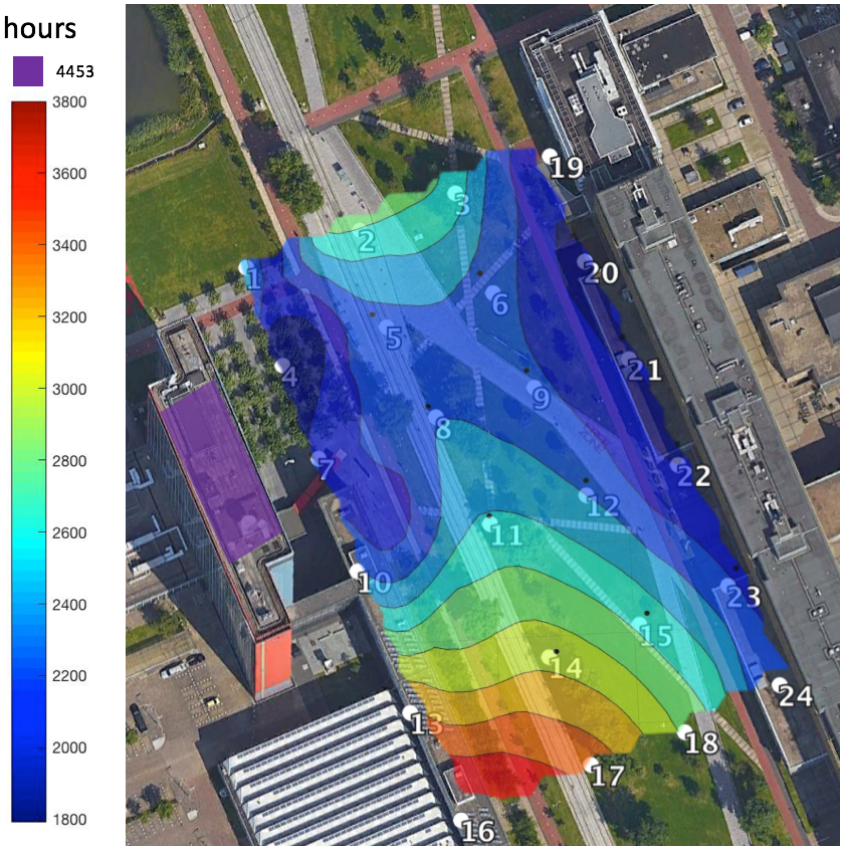

Figure 27: Cubic interpolation of calculated sunlight hours

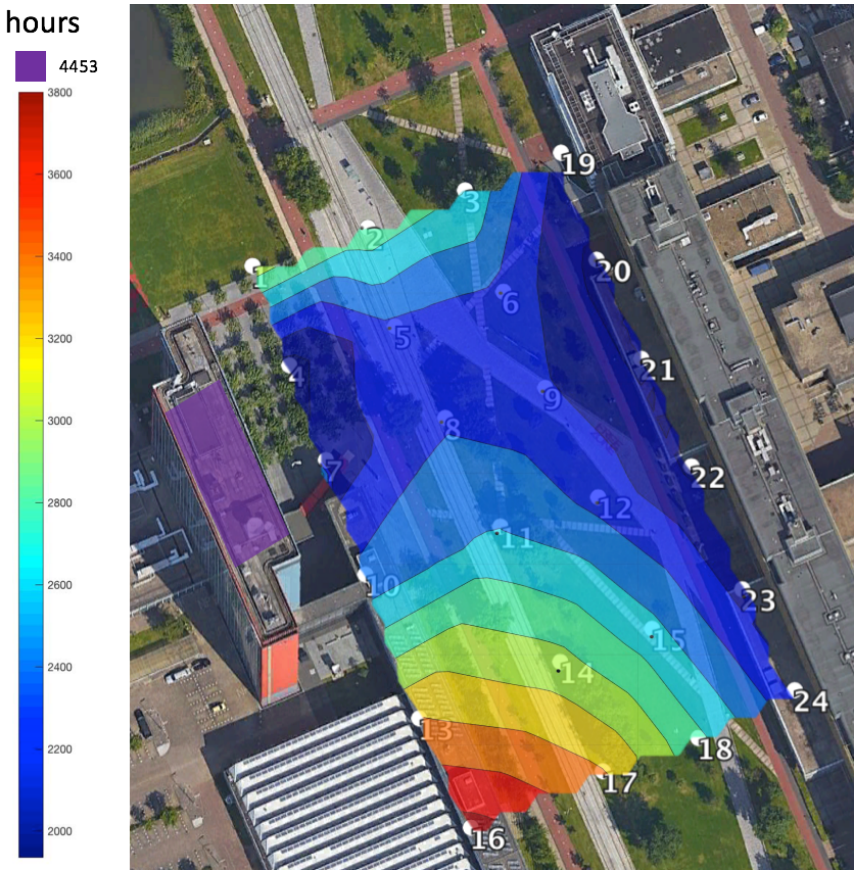

Figure 28: Linear interpolation of calculated sunlight hours

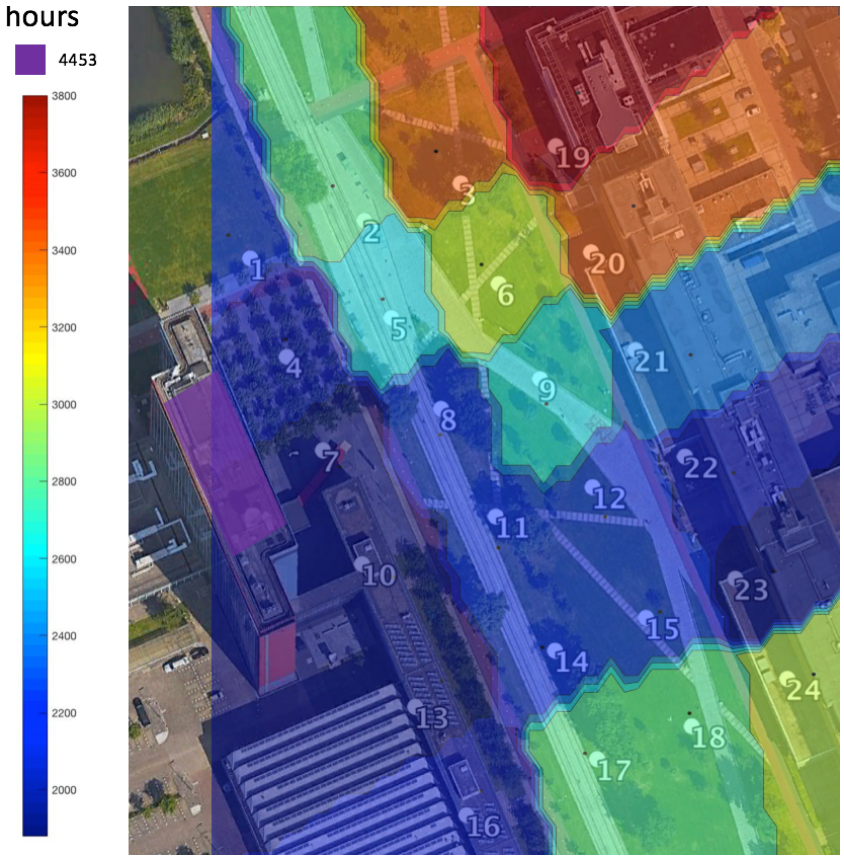

Figure 29: Nearest-Neighbour interpolation of calculated sunlight hours

Since all three interpolation methods used here are exact, a numerical analysis with sum squares of residuals can't be applied. A valid assessment, however, can be made if we perform cross-validation. This involves leaving out a point for the interpolation and comparing this with the results obtained with all data points. This can be efficiently done with the curve fitting tool in Matlab, using the Exclude Outliers function. In figure 30, the results of the linear interpolation, using cross-validation can be seen. The first image in the figure shows the linear interpolation results including all data points, while the second and third images show the results after the exclusion of data points 9 and 12, respectively. This cross validation was also preformed with the cubic interpolation and the changes were more significant than those visible in figure 30 for the linear interpolation.

The Nearest-Neighbour interpolation seems to be displaying some weird results, in the strange thin line around certain sections of the interpolation. This strange behaviour was due to some Matlab code problems, which unfortunately could not be fixed. In light of the cross validation performed with linear and cubic interpolation and the issue with the Nearest-Neighbour interpolation, the linear interpolation method will be used during the remained of the calculations.

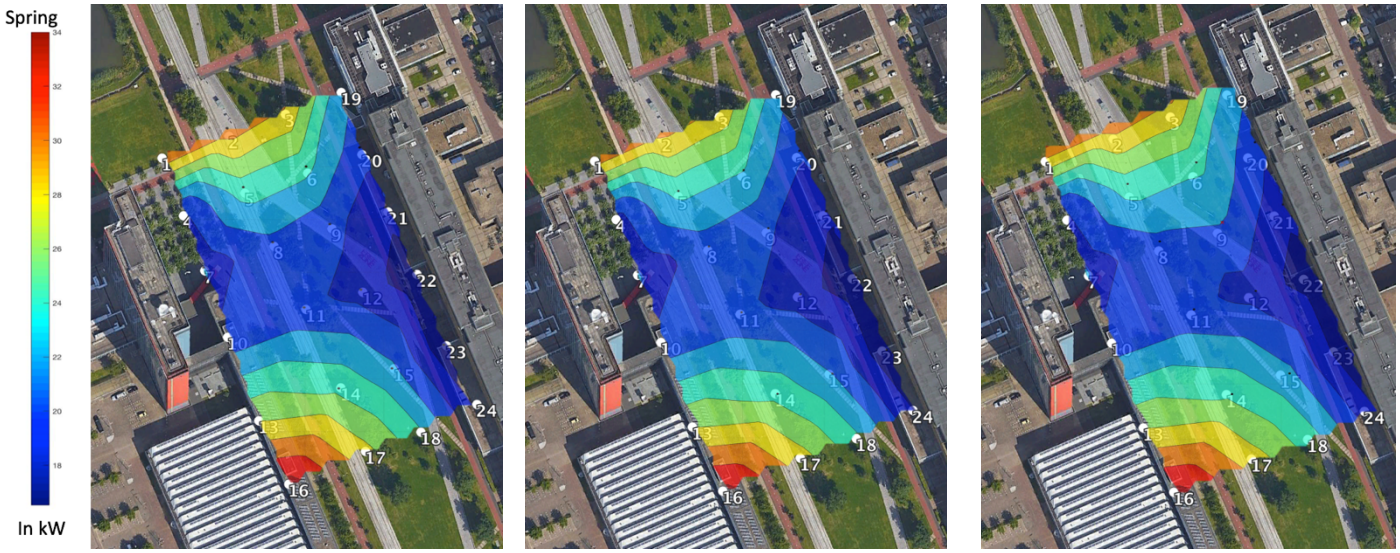

Figure 30: Results of the linear interpolation, using cross-validation. The first image shows the linear interpolation results including all data points, while the second and third images show the results after the exclusion of data points 9 and 12, respectively.

Chapter 4.2: Results with Radiation from Weather Data

Using the data from the KNMI obtained in Chapter 3.3, four interpolation maps will be generated in this chapter.

First the hourly results per day from Chapter 4.1 were multiplied by the radiation data in W*h, thus calculating the amount of Watts generated per day. These days were subsequently split into sections based on the four astronomical seasons (spring, summer, autumn and winter astronomical seasons use the dates of equinoxes and solstices to mark the beginning and end of seasons in a year. In figures 30 & 31, the average amount of kW generated per day in each of the seasons over the area of the park is displayed. In figure 30, the colour bar is not constant throughout all four seasons to provide a more detailed look at the results. Figure 31 is more

useful for comparison purposes between the seasons, since the colour bar is constant for all the maps. A different colour scheme was also chosen to highlight the differences more.

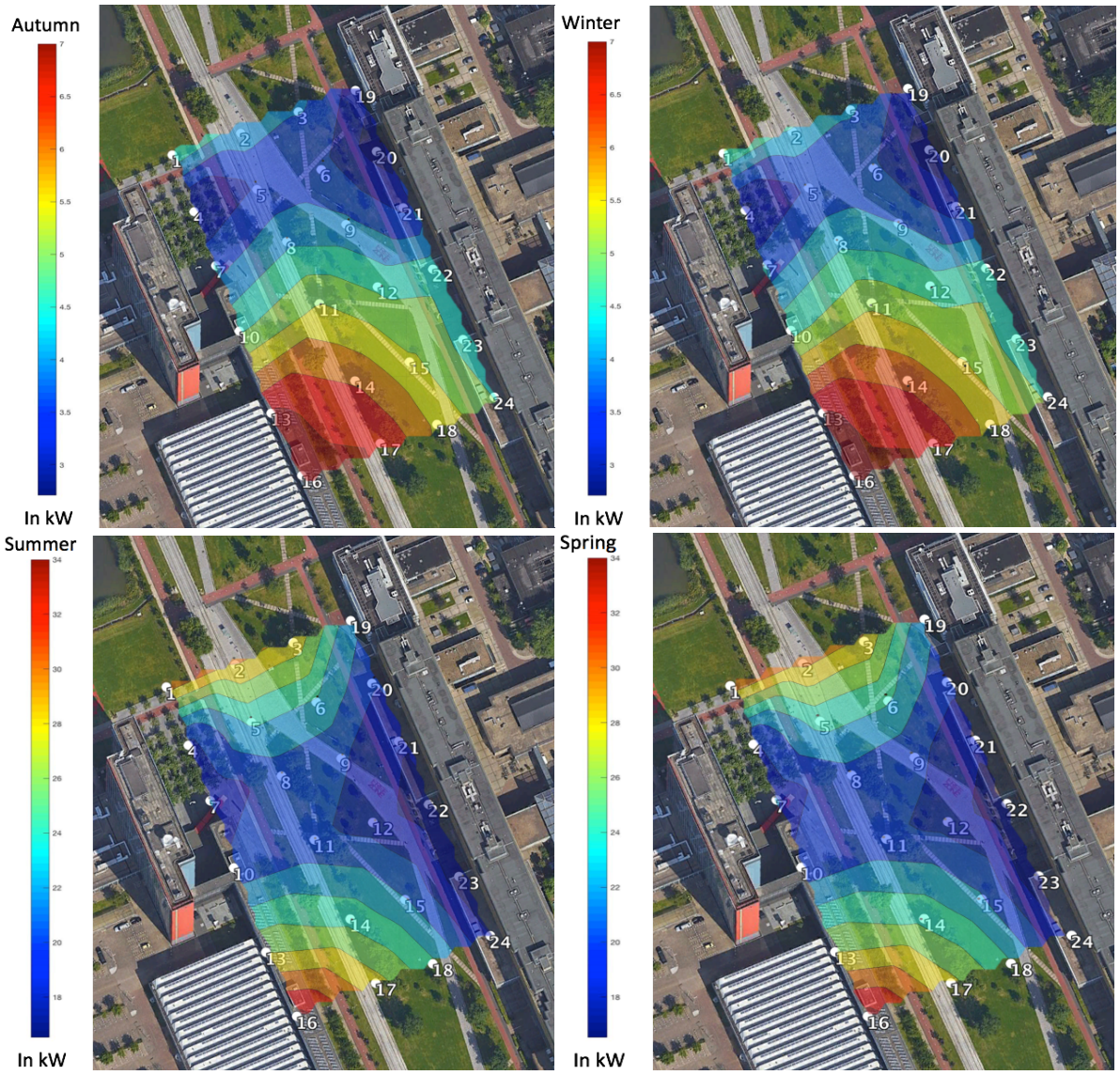

Figure 30: Linear interpolation of calculated sunlight kW intensity for each of the four seasons.

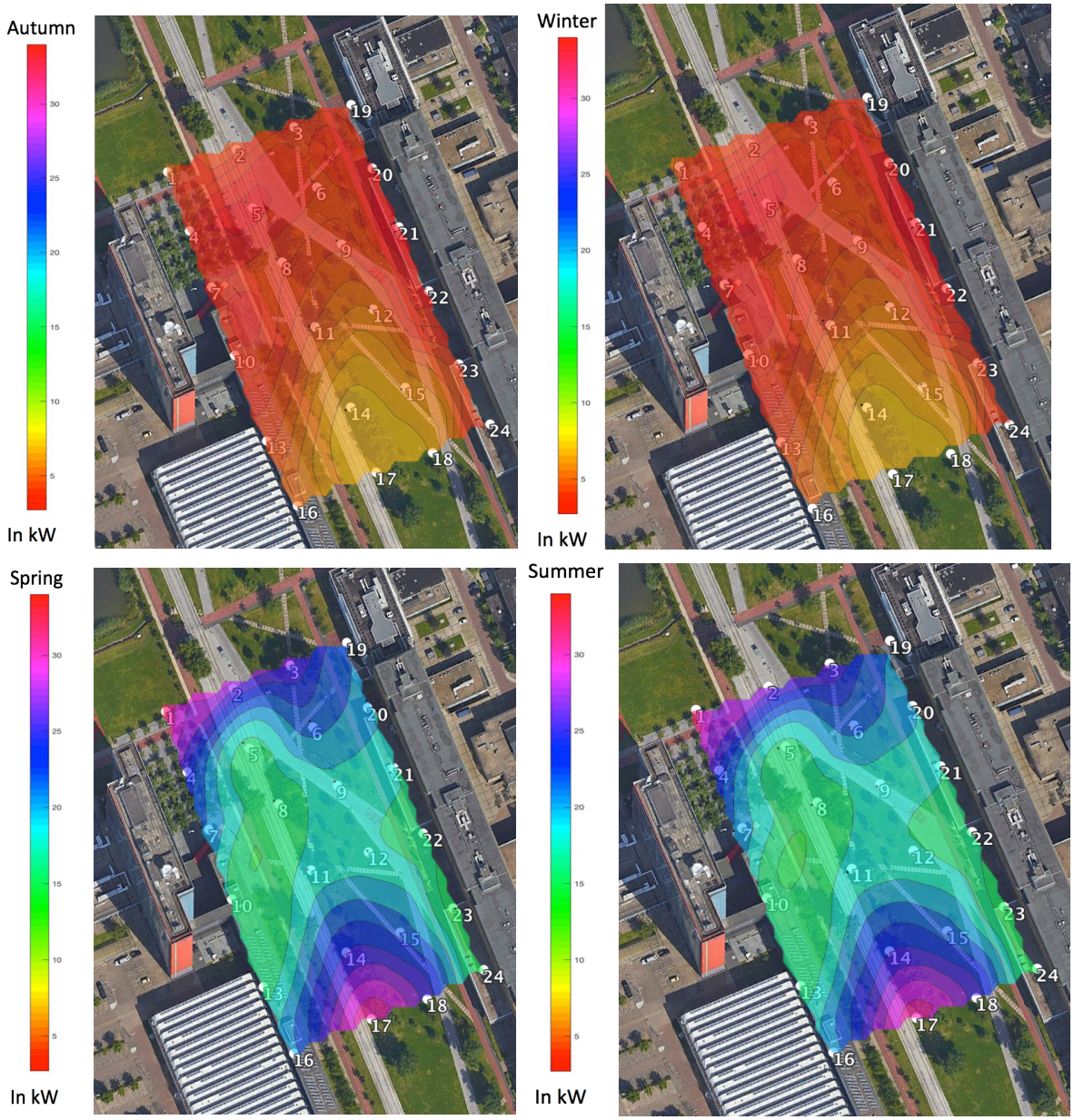

Figure 31: Linear interpolation of calculated sunlight kW intensity for each of the four seasons, with the same color bar.

Several seasonal dependent effects are visible in these final results. As calculated in Chapter 3.2, in the winter and autumn the Sun doesn't reach as far up in the sky as in the Spring and Summer months (see figures 14 & 15). This effect, in combination with the lower radiation values during the winter and autumn months contribute to the large difference in average kW per day between the winter/autumn and summer/spring.

In table 2 the reference without shadow was also calculated, making the seasonal effect clearly visible.

Table 2	
Season	**kW on average per day without shadow effect**
Autumn	25.71
Winter	25.82
Spring	36.92
Summer	36.53

Table 2: the reference with zero shadow

The total amount of kW produced over the entire year was also calculated. This was done by adding the values per day of each season together. This resulted in a value of $1.35*10^3$ kW for the entire year if 24 solar panels of a size of 200 cm^2 is placed on the 24 specified site in the Mekelpark.

6 streetlamps are a realistic estimate over the area of 0.04 km^2 in the Mekelpark (estimated from a visual assessment made at the site). The Mekelpark currently doesn't need a denser placement of streetlamps. If we assume a single simple light bulb is around 200 W, this means a single light can be eliminated for $6.73*10^3$ hours ≈ 280 days, and 6 streetlamps can be illuminated for:

$$\frac{1.3469*10^6\ W}{200\ W*6\ bulbs} \approx 46.7 \text{ full days} \approx 93\ nights.$$

Chapter 4.3: Discussion

Various assumptions were made to make these solar potential calculations possible. In this chapter these assumptions and their impacts will be discussed.

The first assumptions are in relation to the geometry of the Mekelpark. This is where the biggest error will arise in the calculation of the solar potential, since the geometry has the biggest impact. As can be seen in figure 7 and figure 9, in the Mekelpark some trees are present. These trees, have a height of around 4 meters. This was determined from the height data (see Chapter 3.1). Since the light poles have a height of around 2 meters, these trees could block a significant amount of sunlight from reaching the solar panels on the light posts. The leafage of these trees, which also varies per season, are an important factor that need to be taken into account when the solar potential is calculated. During the winter, the leafage amount will be at a minimum, which is fortunate, since during this time the most solar energy will need to be collected and

leafage could hinder this collecting of energy. During the summer and spring, the leafage will be maximum and hindering the solar energy that can be harvested.

Another geometry characteristic, that can be seen in figure 7 and figure 9, is the relief in elevation present in the Mekelpark. This wave-like pattern travels the North-South direction of the park with a maximum elevation difference from a reference height of 2.5 meters. So this will not have a large impact on a direct shadow on the lampposts, since the height difference isn't that high, like with the trees. However, if the lampposts are placed on these elevations, they have a higher possibility to 'catch' more solar potential.

Another assumption is related to the shape of the solar panels. The model of the solar panels that was used in the calculations were assumed to be a horizontal flat surface with an area of 200 cm^2. However, the actual solar panels are wrapped around the light pole. This has an impact on the area of the solar panels and thus their potential. But this wrapping also causes a difference of the potential energy that is gathered throughout the day, since when one end of the pole can be in the sunlight, the opposite end of the pole won't be in the sunlight and won't harvest any energy. This will have a large impact the estimated solar potential.

Data from several sources was used for the calculations of the estimated solar potential. The errors of this data should also be taken into consideration for the accuracy of the estimation.

The KNMI data, which was used for the determination of the radiation. This data is for the entire Netherlands, so for a more reliable result, the radiation should be determined for Delft or the Mekelpark, specifically.

The formulas used for the calculation of the Sun's position were taken from the book: Astronomical Algorithms[28]. They are theoretically accurate to within a minute for location between +/- 72° latitude and within 10 minutes outside of those latitudes. Since our location falls between this +/- 72° latitude, an accuracy of one minute for the Sun azimuth and elevation for each hour can be expected. This effect won't have a large impact on the accuracy of the calculations of the solar potential.

These formulas[28], also don't include the effects of various phenomena, which could impact the amount of sun-time. These phenomena include; atmospheric composition, temperature and pressure. This won't have a large impact on the accuracy of the calculations of the solar potential, either.

Chapter 5: Conclusion & Recommendations

Conclusions

We can conclude from this report on investigating the solar potential of the Mekelpark, that FlexSols solar panel street lamps are certainly an option at this location. The amount of solar potential generated over an entire year for 24 solar panels was determined to be $1.35*10^3$ kW. This is assuming that the solar panels have an efficiency of 100%, which is not the case. This constraint is, of course, dependent on the manufacture of the solar panel and is data that can be collected from FlexSol.

As was anticipated the kW per day varies throughout the seasons, not only because the Sun intensity varies, but because the Sun doesn't reach as high throughout the year. As a result of sunlight hour calculations, the percentage hours of sunlight compared to a shadow-less location range from 42% to 88%. For the results of the kW per day as a percentage of a shadow less location, ranges from 33% to 40%.

Recommendations

The KNMI website monthly overviews are only available from 2009 to 2017. To make a more reliable model, in the Addition of Weather Factor chapter, this could be extended to include more year, however, the KNMI would have to be contacted for this, since this information is not on their website.

The KNMI data, which was used for the determination of the radiation, is data for the entire Netherlands. These measurements are done with a pyranometer (as discussed in Chapter 3.3). For a more reliable estimation of the radiation, measurements with a pyranometer should be performed at the investigated site, in this case the Mekelpark.

As observed in the discussion the geometry (trees and height differences) of the Mekelpark should be taken into account for a more accurate solar potential estimation. The shape of the solar panel should also be incorporated into the calculations for a more accurate solar potential estimation.

In this report an over simplified version of the site was assumed for the calculations. Working with point clouds would give a more realistic result for the specific location of the Mekelpark, since more complex shapes in buildings can be used for shadow calculations. In these point clouds, trees and elevation differences, as introduced in the discussion, can also be taken into account for the calculations.

Another issue, not discussed in this report is the fact that the time of year when street lighting is needed most (during the longer nights of winter and fall), the least energy will be generated by the streetlamps. A solution to this problem should also be found, for example; decreasing the lamp's luminosity during this time, since storage of energy is a complex process.

References

1. https://www.tudelft.nl/sustainability/ (last visited on 21 Oct 2017)
2. Nguyen H T, Pearce J M, Harrap R, et al. (2012) The Application of LIDAR To Assessment Of Rooftop Solar Photovoltaic Deployment Potential In A Municipal District Unit. Sensors 12: 4534–4558.
3. Redweik, P.; Catita, C.; Brito, M. (2013) Solar Energy Potential On Roofs and Facades in an Urban Landscape. Sol. Energy, 97, 332–341.
4. A. Jochem, B. Hofle, M. Rutzinger and N. Pfeifer (2009). Automatic Roof Plane Detection and Analysis in Airborne Lidar Point Clouds for Solar Potential Assessment. From Department of Geography University of Innsbruck.
5. J.B. Campbell. (1996). Introduction to Remote Sensing. Taylor & Francis, London.
6. http://atropos.as.arizona.edu/aiz/teaching/a204/images/em_spec.gif (last visited on 21 Oct 2017)
7. Fröhlich, C., and R. W. Brusa (1981), "Solar Radiation and its Variation in Time", Solar Physics 74, 209.
8. Iqbal, M. (1983), An Introduction to Solar Radiation, Academic Press, New York.
9. "Quantum States of Atoms and Molecules" by David M. Hanson, Erica Harvey, Robert Sweeney, Theresa Julia Zielinski
10. https://swcphysics30.wordpress.com/2012/06/09/the-photoelectric-effect-and-power-generation-from-solar-energy/solar3-2/ (last visited on 21 Oct 2017)
11. http://www.ahn.nl/index.html (last visited on 21 Oct 2017)
12. Fraunhofer Institute: 2015. Photovoltaics report.
13. International Energy Agency (IEA). 2014. Technology roadmap: Concentrating solar power. Paris, France.
14. http://zebu.uoregon.edu/2001/ph162/l7.html (last visited on 21 Oct 2017)
15. https://upload.wikimedia.org/wikipedia/commons/thumb/f/f7/Azimuth-Altitude_schematic.svg/436px-Azimuth-Altitude_schematic.svg.png (last visited on 21 Oct 2017)
16. https://www.esrl.noaa.gov/gmd/grad/alc/azelzen.gif (last visited on 21 Oct 2017)
17. http://suncalc.net/ (last visited on 21 Oct 2017)
18. https://www.esrl.noaa.gov/gmd/grad/solcalc/azel.html (last visited on 21 Oct 2017)
19. http://www.ucsusa.org/clean-energy/renewable-energy/solar-power-plants-large-scale-

pv#.WaU3W62B3ok (last visited on 21 Oct 2017)
20. https://www.texasgateway.org/resource/electromagnetic-spectrum-introduction (last visited on 21 Oct 2017)
21. http://www.slate.com/blogs/bad_astronomy/2013/04/29/analemma_the_position_of_the_sun_in_the_sky_changing_over_a_year.html (last visited on 21 Oct 2017)
22. W.G. Rees (2013) Physicals Principles of Remote Sensing
23. "Solar Energy Systems Design" by W.B. Stine and R.W. Harrigan (John Wiley and Sons, Inc. 1986)
24. https://www.knmi.nl/nederland-nu/klimatologie/gegevens/mow (last visited on 21 Oct 2017)
25. https://earthobservatory.nasa.gov/Features/Clouds/ (last visited on 21 Oct 2017)
26. http://www.knmi.nl/nederland-nu/klimatologie/geografische-overzichten/archief/maand/sq (last visited on 21 Oct 2017)
27. http://support.esri.com/en/technical-article/000005606 (last visited on 21 Oct 2017)
28. Astronomical Algorithms by Jean Meeus (1991)
29. https://commons.wikimedia.org/wiki/File:Comparison_of_1D_and_2D_interpolation.svg (last visited on 21 Oct 2017)
30. Li, D.; Liu, G.; Liao, S. Solar Potential in Urban Residential Buildings. Solar Energy 2015, 111, 225–235 DOI: 10.1016/j.solener.2014.10.045.

Appendix A.1

First, the amount of hours of Sun at a single location will be calculated, according to the geometry of the situation (this was done in the suncalculation section) and the position of the Sun (in the Sun_position section). The comparison of these was done in the Matching both calculations section). This should be performed for all of the 24 points. Then, using KNMI data, this calculation will be adjusted for average weather conditions (in the Creating a Curve fitting model with Weather conditions section). This will generate a model of the expected kW per day for an area of the Mekelpark.

```
%Suncalculation
clear all
azimuth=[0:1:359]';
format short g;
beta=1;
gamma = zeros(360, 1);
alpha = zeros(360, 1);
xbuilding = zeros(360, 1);
altitue_angle_building = zeros(360, 1);
gamma(1)=0;
alpha(1)=0;
xbuilding(1)=100;
gamma1=24.20;
gamma(2)=gamma1;
alpha(2)=180-gamma1-beta;
for i=3:360
   for n=2:360
      for j=1:30
         for k=45:58
   gamma(i,1)=180-alpha(i-1);
   alpha(i,1)=180-beta-gamma(i);
   xbuilding(n,1)=(xbuilding(n-1)*sind(gamma(n)))/sind(alpha(n));
   altitue_angle_building(j)=atand(30/xbuilding(j));
   altitue_angle_building(k)=abs(atand(90/xbuilding(k)));
         end
      end
   end
end
```

```
%Sun_position
clear all
latitude=51.9994;
longitude=4.3742;
timezone=1;
date1=42736:1:43100;
date=date1.';
time1=0:1/24:1;
time=time1.';
X=zeros(24,365);
Y=zeros(24,365);
Z=zeros(24,365);
for n=1:24;
   i=1:numel(date1);
Julianday(n,i)=date(i)+2415018.5+time(n)-(timezone/24);


JulianCentury(n,i)=(Julianday(n,i)-2451545)./36520;
Geom_Mean_Long_Sun(n,i)=mod(280.46646+(JulianCentury(n,i)*36000.76983)+((JulianCentury(n,i).^2).*0.0
003032),360);


Geom_Mean_Long_Sunrad(n,i)=((Geom_Mean_Long_Sun(n,i)*pi)./180)';


Geom_Mean_Anom_Sun(n,i)=357.52911+(JulianCentury(n,i)*35999.05029)-
(0.0001537*(JulianCentury(n,i).^2));


eccent_earth_orbit(n,i)=0.016708634-
(JulianCentury(n,i)*0.000042037)+(0.0000001267*JulianCentury(n,i).^2);


eccent_earth_orbitrad(n,i)=(eccent_earth_orbit(n,i)*pi)/180;


Geom_Mean_Anom_Sunrad(n,i)=(Geom_Mean_Anom_Sun(n,i)*pi)/180;


Sun_Eq_of_Ctr(n,i)=sin(Geom_Mean_Anom_Sunrad(n,i)).*(1.914602-
JulianCentury(n,i).*(0.004817+0.000014.*JulianCentury(n,i)))+sin((2*Geom_Mean_Anom_Sunrad(n,i))).*(0.0
19993-0.000101.*JulianCentury(n,i))+sin((3*Geom_Mean_Anom_Sunrad(n,i)))*0.000289;


Sun_True_Long(n,i)=Geom_Mean_Long_Sun(n,i)+Sun_Eq_of_Ctr(n,i);


Sun_App_Long(n,i)=Sun_True_Long(n,i)-0.00569-0.00478*sin((125.04-1934.136*JulianCentury(n,i)));
```

```
Mean_Obliq_Ecliptic(n,i)=23+(26+((21.448-JulianCentury(n,i).*(46.815+JulianCentury(n,i).*(0.00059-
JulianCentury(n,i).*0.001813))))/60)/60;


Obliq_Corr(n,i)=Mean_Obliq_Ecliptic(n,i)+0.00256*cos((125.04-1934.136*JulianCentury(n,i)));
      Sun_Declin(n,i)=(asind(sind((Obliq_Corr(n,i))).*sind(Sun_App_Long(n,i))));


Obliq_Corrrad(n,i)=(Obliq_Corr(n,i)*pi)/180;


var_y(n,i)=tan(Obliq_Corrrad(n,i)/2).*tan(Obliq_Corrrad(n,i)/2);


Eq_of_Time(n,i)=(var_y(n).*sin(2*(Geom_Mean_Anom_Sun(n,i)))-
(2*var_y(n,i).*sin((Geom_Mean_Anom_Sun(n,i)))+(4*eccent_earth_orbit(n,i).*var_y(n,i).*sin(Geom_Mean_A
nom_Sun(n,i)).*cos(2.*(Geom_Mean_Anom_Sun(n,i)))-
(0.5.*var_y(n,i).^2.*sin(4.*Geom_Mean_Anom_Sun(n,i))));


Eq_of_Timedeg(n,i)=4*(Eq_of_Time(n,i)*180)/pi;


True_Solar_Time(n,i)=mod(time(n)*1440+Eq_of_Time(n,i)+4*longitude-60*timezone,1440);


if True_Solar_Time(n,i)/4<0
   Hour_Angle(n,i)=(True_Solar_Time(n,i)/4)+180;
end


if True_Solar_Time(n)/4>0
   Hour_Angle(n,i)=(True_Solar_Time(n,i)/4)-180;
end


Solar_Zenith_Angle1(n,i)=sind(latitude).*sind(Sun_Declin(n,i))+(cosd(latitude).*cosd(Sun_Declin(n,i)).*cosd(
Hour_Angle(n,i)));


Solar_Zenith_Angle3(n,i)=acosd(Solar_Zenith_Angle1(n,i));


Solar_Elevation_Angle(n,i)=90-Solar_Zenith_Angle3(n,i);


if Hour_Angle(n,i)>0
        Solar_Azimuth_Angle(n,i)=acosd(((sind(latitude).*cosd(Solar_Zenith_Angle3(n,i)))-
sind(Sun_Declin(n,i)))/(cosd(latitude).*sind(Solar_Zenith_Angle3(n,i))))+180;
         else Solar_Azimuth_Angle(n,i)=mod(540-acosd(((sind(latitude).*cosd(Solar_Zenith_Angle3(n,i)))-
sind(Sun_Declin(n,i)))/(cosd(latitude).*sind(Solar_Zenith_Angle3(n,i)))),360);
         end
end
```

```
figure(1)
k = 5;
n = 2^k-1;
theta = pi*(-n:2:n)/n;
phi = (pi/2)*(0:2:n)'/n;
X = cos(phi)*cos(theta);
Y = cos(phi)*sin(theta);
Z = sin(phi)*ones(size(theta));
surf(X,Y,Z,'FaceColor', 'white','FaceAlpha',0.5);
hold on


for i=1:30:335

scatter3(cosd(Solar_Elevation_Angle(1:24,i)).*cosd(Solar_Azimuth_Angle(1:24,i)),cosd(Solar_Elevation_Angle(1:24,i)).*sind(Solar_Azimuth_Angle(1:24,i)),sind(Solar_Elevation_Angle(1:24,i)).*ones(size(Solar_Azimuth_Angle(1:24,i))), 'filled');

line(cosd(Solar_Elevation_Angle(1:24,i)).*cosd(Solar_Azimuth_Angle(1:24,i)),cosd(Solar_Elevation_Angle(1:24,i)).*sind(Solar_Azimuth_Angle(1:24,i)),sind(Solar_Elevation_Angle(1:24,i)).*ones(size(Solar_Azimuth_Angle(1:24,i))));
   labels = num2str((1:size(time)-1)','%d');
   axis([-1 1, -1 1, 0 1])
end


%Matching both calculations
A = Solar_Elevation_Angle;
B = Solar_Azimuth_Angle;
C = B(:,[1;1]*(1:size(B,2)));
C(:,1:2:end) = A;
combo=round(C);
AzimuthD=zeros(24,365);
ElevationD=zeros(24,365);
D=zeros(24,730);
Solar_Elevation_Angle(Solar_Elevation_Angle<0)=0; %everything below horizon = 0
%Reshape A into 2-columns matrix (called Ar) to avoid having to use nested for loops later
Ar = reshape([combo(:, 1:2:end) combo(:, 2:2:end)], numel(combo)/2, 2);
%R will store value = 1 if conditions are met, value = 0 if conditions fail
R = zeros(size(Ar, 1), 1);
for k = 1:size(Ar, 1)
   %if azimuth and elevation in Ar is greater than ANY from B, change R(k) to 1
   if any( Ar(k, 1) >= neededround(:, 1) & Ar(k, 2)==neededround(:, 2))
```

```
        R(k) = 1;
    end
end
% %Number of times conditions are met per hour (row) for all day (col)
R = reshape(R, size(combo, 1), size(combo, 2)/2);
% %Number of times conditions are met per day
Rday = sum(R, 1);
% %Number of times conditions are met per year
Ryear = sum(Rday);


%Creating a Curve-fitting model
Ryearint=[Ryear1 Ryear2 Ryear3 Ryear19; Ryear4 Ryear5 Ryear6 Ryear20; Ryear7 Ryear8 Ryear9 Ryear21;
Ryear10 Ryear11 Ryear12  Ryear22; Ryear13 Ryear14 Ryear15 Ryear23; Ryear16 Ryear17 Ryear18 Ryear24];
x= [51.999458 51.999544 51.999631 51.999714; 51.999233 51.999322 51.999400 51.999472; 51.999019
51.999114 51.999183 51.999247; 51.998761 51.998869 51.998936 51.999006; 51.998436  51.998564
51.998639 51.998728; 51.998189 51.998317 51.998392 51.998500;];
y= [4.373586 4.374008 4.374364 4.374717; 4.373722 4.374108 4.374506 4.374847; 4.373858 4.374294
4.374658 4.375011; 4.374003 4.374494 4.374853 4.375194; 4.374197 4.374714 4.375050 4.375381; 4.374386
4.374869 4.375219 4.375572;];


Vq =  cftool(x,y,Ryearint);


% Creating a Curve fitting model with Weather conditions
dayshour= [Rday1; Rday2 ; Rday3; Rday4; Rday5; Rday6; Rday7; Rday8; Rday9; Rday10; Rday11; Rday12;
Rday13; Rday14; Rday15; Rday16; Rday17; Rday18; Rday19; Rday20; Rday21; Rday22; Rday23; Rday24;];


Janwh = 7831*(2.7778*10.^-7)*200;  %J/cm2 to kWh
Febwh = 12677*(2.7778*10.^-7)*200;
Marwh = 29729*(2.7778*10.^-7)*200;
Aprwh = 45928*(2.7778*10.^-7)*200;
Maywh = 56008*(2.7778*10.^-7)*200;
Junwh = 58105*(2.7778*10.^-7)*200;
Julwh = 57807*(2.7778*10.^-7)*200;
Augwh = 50703*(2.7778*10.^-7)*200;
Sepwh = 33722*(2.7778*10.^-7)*200;
Octwh = 19453*(2.7778*10.^-7)*200;
Novwh = 8720*(2.7778*10.^-7)*200;
Decwh = 5943*(2.7778*10.^-7)*200;


daysWJ=dayshour(:,1:31)*Janwh;
```

```
daysWF=dayshour(:,32:59)*Febwh;

daysWM=dayshour(:,60:90)*Marwh;

daysWA=dayshour(:,91:120)*Aprwh;

daysWMay=dayshour(:,121:151)*Maywh;

daysWJun=dayshour(:,152:181)*Junwh;

daysWJul=dayshour(:,182:212)*Julwh;

daysWAug=dayshour(:,213:243)*Augwh;

daysWSep=dayshour(:,244:273)*Sepwh;

daysWOct=dayshour(:,274:304)*Octwh;

daysWNov=dayshour(:,305:334)*Novwh;

daysWDec=dayshour(:,335:365)*Decwh;


dayW= [daysWJ daysWF daysWM daysWA daysWMay daysWJun daysWJul daysWAug daysWSep
daysWOct daysWNov daysWDec];

totwpoint=[ sum(dayW(1,:)) sum(dayW(2,:)) sum(dayW(3,:)) sum(dayW(4,:)) sum(dayW(5,:)) sum(dayW(6,:))
sum(dayW(7,:)) sum(dayW(8,:)) sum(dayW(9,:)) sum(dayW(10,:)) sum(dayW(11,:)) sum(dayW(12,:))
sum(dayW(13,:)) sum(dayW(14,:)) sum(dayW(15,:)) sum(dayW(16,:)) sum(dayW(17,:)) sum(dayW(18,:))
sum(dayW(19,:)) sum(dayW(20,:)) sum(dayW(21,:)) sum(dayW(22,:)) sum(dayW(23,:)) sum(dayW(24,:))];


averagewinter=mean([dayW(:,355:end) dayW(:,1:79)],2)

averagespring=mean(dayW(:,80:172),2)

averagesummer=mean(dayW(:,173:264),2)

averageautumn=mean(dayW(:,265:355),2)


KWsping=[averagespring(1,1) averagespring(2,1) averagespring(3,1) averagespring(19,1); averagespring(4,1)
averagespring(5,1) averagespring(6,1) averagespring(20,1); averagespring(7,1) averagespring(8,1)
averagespring(9,1) averagespring(21,1); averagespring(10,1) averagespring(11,1) averagespring(12,1)
averagespring(22,1); averagespring(13,1) averagespring(14,1) averagespring(15,1) averagespring(23,1);
averagespring(16,1) averagespring(17,1) averagespring(18,1) averagespring(24,1)];


KWwinter=[averagewinter(1,1) averagewinter(2,1) averagewinter(3,1) averagewinter(19,1); averagewinter(4,1)
averagewinter(5,1) averagewinter(6,1) averagewinter(20,1); averagewinter(7,1) averagewinter(8,1)
averagewinter(9,1) averagewinter(21,1); averagewinter(10,1) averagewinter(11,1) averagewinter(12,1)
averagewinter(22,1); averagewinter(13,1) averagewinter(14,1) averagewinter(15,1) averagewinter(23,1);
averagewinter(16,1) averagewinter(17,1) averagewinter(18,1) averagewinter(24,1)];


KWsummer=[averagesummer(1,1) averagesummer(2,1) averagesummer(3,1) averagesummer(19,1);
averagesummer(4,1) averagesummer(5,1) averagesummer(6,1) averagesummer(20,1); averagesummer(7,1)
averagesummer(8,1) averagesummer(9,1) averagesummer(21,1); averagesummer(10,1) averagesummer(11,1)
averagesummer(12,1) averagesummer(22,1); averagesummer(13,1) averagesummer(14,1) averagesummer(15,1)
averagesummer(23,1); averagesummer(16,1) averagesummer(17,1) averagesummer(18,1)
averagesummer(24,1)];


KWautumn=[averageautumn(1,1) averageautumn(2,1) averageautumn(3,1) averageautumn(19,1);
averageautumn(4,1) averageautumn(5,1) averageautumn(6,1) averageautumn(20,1); averageautumn(7,1)
```

```
averageautumn(8,1) averageautumn(9,1) averageautumn(21,1); averageautumn(10,1) averageautumn(11,1)
averageautumn(12,1) averageautumn(22,1); averageautumn(13,1) averageautumn(14,1) averageautumn(15,1)
averageautumn(23,1); averageautumn(16,1) averageautumn(17,1) averageautumn(18,1) averageautumn(24,1)];


x= [51.999458 51.999544 51.999631 51.999714; 51.999233 51.999322 51.999400 51.999472; 51.999019
51.999114 51.999183 51.999247; 51.998761 51.998869 51.998936 51.999006; 51.998436  51.998564
51.998639 51.998728; 51.998189 51.998317 51.998392 51.998500;];


y= [4.373586 4.374008 4.374364 4.374717; 4.373722 4.374108 4.374506 4.374847; 4.373858 4.374294
4.374658 4.375011; 4.374003 4.374494 4.374853 4.375194; 4.374197 4.374714 4.375050 4.375381; 4.374386
4.374869 4.375219 4.375572;];


for i=1:18
   Vq =  cftool(x,y,KWsping);
end
```

Appendix A.2

This appendix contains the full KNMI data introduced in Chapter 3.3 and used in the radiation calculations in chapter 4.2. This data is from 2017 to 2009.

Monthly KNMI Data							
	Sunshine Duration (hours)	Percentage (%)	Radiation (J/cm^2)		Sunshine Duration (hours)	Percentage (%)	Radiation (J/cm^2)
Jan-17	87,3	34	8940	Feb-17	70,6	25	11271
Jan-16	69,8	27	7631	Feb-16	105,7	37	14814
Jan-15	67,7	26	7470	Feb-15	110,7	40	14993
Jan-14	68,7	27	7604	Feb-14	100,8	36	13767
Jan-13	59,9	23	7318	Feb-13	81,6	29	12547
Jan-12	69,7	27	7479	Feb-12	113,3	39	15061
Jan-11	67,1	26	7496	Feb-11	65,7	24	10840
Jan-10	62	24	7572	Feb-10	57,2	21	10650
Jan-09	95,1	37	8970	Feb-09	52,3	19	10152
Mar-17	177,6	48	31554	Apr-17	200,4	48	45236
Mar-16	147,8	40	28109	Apr-16	194,5	47	44116
Mar-15	157,8	43	28199	Apr-15	241,1	58	49533
Mar-14	208,2	57	34374	Apr-14	179,7	43	42686
Mar-13	126	34	26823	Apr-13	193,6	46	44672
Mar-12	166	45	29875	Apr-12	150,1	36	37983
Mar-11	185,1	50	32004	Apr-11	262,1	63	51085
Mar-10	151,8	41	28477	Apr-10	245,7	59	50754
Mar-09	151,5	41	28150	Apr-09	226,2	54	47287
May-17	231,5	47	58601	Jun-17	231,2	46	59926
May-16	232,3	48	58156	Jun-16	162,8	33	50612
May-15	222,4	46	57000	Jun-15	241,3	48	61948
May-14	208,8	43	53846	Jun-14	226,8	46	60687
May-13	177,9	37	48533	Jun-13	184,4	37	53765
May-12	219,1	45	55908	Jun-12	178,2	36	51498
May-11	265,5	55	61346	Jun-11	217,3	43	56180
May-10	199,7	41	51867	Jun-10	264,8	53	64841
May-09	247,4	51	58814	Jun-09	248,4	50	63489
Jul-17	206,5	41	56793	Aug-17	197,2	43	47867
Jul-16	223,6	45	58139	Aug-16	240,1	53	63290
Jul-15	224,3	45	57173	Aug-15	219	48	51011
Jul-14	221,6	44	57171	Aug-14	202,9	45	47116

	Sunshine Duration (hours)	Percentage (%)	Radiation (J/cm^2)		Sunshine Duration (hours)	Percentage (%)	Radiation (J/cm^2)
Jul-13	254,7	51	63290	Aug-13	233,8	51	53095
Jul-12	208,1	41	55534	Aug-12	232,6	51	53357
Jul-11	158	31	48854	Aug-11	153,3	34	43155
Jul-10	257,3	51	63512	Aug-10	169,9	37	43413
Jul-09	239,6	48	59793	Aug-09	240,6	53	54022
Sep-16	217,1	57	39160	Oct-16	130,6	40	20315
Sep-15	156,8	41	32009	Oct-15	114,6	35	19124
Sep-14	177,7	47	35385	Oct-14	109,3	33	18192
Sep-13	147	39	31962	Oct-13	117,8	36	19437
Sep-12	174,6	46	34587	Oct-12	108,8	33	18143
Sep-11	161,8	43	32590	Oct-11	153,5	46	21384
Sep-10	141,1	37	30592	Oct-10	123,4	37	20233
Sep-09	160,8	42	33488	Oct-09	112,9	34	18793
Nov-16	83,1	31	9510	Dec-16	72,3	30	6607
Nov-15	63,3	24	8638	Dec-15	74,8	31	6586
Nov-14	89,2	34	9936	Dec-14	49,9	21	5186
Nov-13	54	20	7959	Dec-13	79,5	33	6762
Nov-12	64,5	24	8382	Dec-12	45,4	19	5214
Nov-11	95	36	10134	Dec-11	51,6	21	5340
Nov-10	49,2	19	7617	Dec-10	50,3	21	5874
Nov-09	53,6	20	7586	Dec-09	59,5	25	5971